Pai, S.G.S. and I. F. C. Smith, "Validating model-based data interpretation methods for quantification of reserve capacity," *Adv. Eng. Informatics*, vol. 47, p. 101231, Jan. 2021.
DOI : https://doi.org/10.1016/j.aei.2020.101231

VALIDATING MODEL-BASED DATA INTERPRETATION METHODS FOR QUANTIFICATION OF RESERVE CAPACITY

Sai G. S. Pai [a,*], Ian F.C. Smith [a,b]

[a] Cyber Civil Infrastructure, Future Cities Laboratory, Singapore-ETH Centre, ETH Zurich, Singapore;
[b] Applied Computing and Mechanics Laboratory, Swiss Federal Institute of Technology (EPFL), Station 18, GC-G1-537, Lausanne, Switzerland

* Corresponding author: Sai G.S. Pai, Email: sai.pai@sec.ethz.ch

Abstract

Optimal performance of civil infrastructure is an important aspect of liveable cities. A judicious combination of physics-based models with monitoring data in a validated methodology that accounts for uncertainties is explored in this paper. This methodology must support asset managers when they need to extrapolate current performance to meet future needs. Three model-based data-interpretation methodologies, residual minimization, Bayesian model updating and error-domain model falsification (EDMF), are compared according to their ability to provide accurate interpretations of monitoring data. These comparisons are made using a full-scale case study, a steel-concrete composite bridge in USA. Validation of data interpretation is carried out using cross-validation (leave-one-out and hold-out). A joint-entropy metric is used to evaluate the extent to which the data that is used for validation contains information that is independent of data used for interpreting structural behaviour. Once accurately updated and validated knowledge of structural behaviour is available, it is employed to make predictions of remaining fatigue-life of the bridge. Validated identification of structural behaviour helps ensure accurate predictions of capacity of bridges beyond their design lives. EDMF and a modified form of Bayesian model updating are analytically and numerically equivalent, while EDMF has several practical

advantages. Both methods provide accurate identification and safe estimations of the remaining fatigue life of the bridge. Such enhanced understanding of structural behaviour leads to appropriate decisions regarding civil infrastructure assets.

Keywords
Structural identification, Bayesian model updating, Model falsification, Cross-validation, Asset management

---

1. INTRODUCTION

Due to increasing urbanization and growth of mega-cities, management of existing civil infrastructure is an important challenge of this century (ASCE 2017). Replacement of all existing infrastructure at the end of their design-service lives is expensive and not sustainable (Drzik 2019; World Economic Forum 2014). Already, the architecture, engineering and construction (AEC) industry is the largest consumer of mined raw materials (Amin and Watkins 2018; World Economic Forum and Boston Consulting Group 2018). Moreover, most existing civil infrastructure elements are designed and built using conservative practices due to high perceived risk. This leads to civil infrastructure that is much safer than design requirements, albeit with unknown additional capacity, which in this paper, is called reserve capacity. Monitoring and interpreting structural response can help improve understanding of structural behaviour and quantify this reserve capacity to enhance decision-making and help avoid unnecessary and expensive actions such as extensive repair and most especially, complete replacement.

Interpreting monitoring data (strain, acceleration, deflections etc.) using physics-based models, such as finite element (FE) models, is an inverse task called structural identification (Moon et al.

2013). The task is ill-posed due to the presence of uncertainties from modelling assumptions and measurement (sensor noise). Accuracy of solutions depends upon good estimations of uncertainties affecting the task of structural identification (Goulet and Smith 2013; Pasquier and Smith 2015). Due to the importance of uncertainties to obtain accurate solutions, many researchers have investigated uncertainty sources (Mottershead and Friswell 1993; Soize 2010, 2012). A summary of uncertainty sources and their categories was provided by Simoen et al. (2015).

Engineering models that have been used to interpret data are conservative (Goulet et al. 2013) approximations of reality (Walker et al. 2003). Civil engineering models have been shown to possess large and biased modelling uncertainties (Goulet and Smith 2013; Pai et al. 2018; Pasquier and Smith 2015), which have to be taken into account during model-based data interpretation.

Residual minimization has been the most popular methodology for data interpretation in practice (Alvin 1997). This methodology implicitly involves the assumption of zero-mean uncertainties and no systematic bias. In the presence of typically conservative modelling assumptions, wrong solutions are likely (Pai et al., 2018; Goulet et al., 2013c; Reuland et al., 2017a).

Bayesian model updating (BMU) (Beck and Katafygiotis 1998) has been used primarily by researchers. In BMU, probability distributions of model parameters are updated using information from data. While employing BMU, uncertainties have been traditionally been defined by zero-mean, Gaussian and independent distributions. When these uncertainty assumptions are not satisfied, the solutions obtained have been shown to be inaccurate (Goulet and Smith 2013; Pasquier and Smith 2015; Simoen et al. 2013).

Few researchers have included the effect of model uncertainty when applying BMU (Kwon et al. 2013; Papadimitriou et al. 2001; Simoen et al. 2015). To incorporate the effect of model

uncertainties in a more rigorous manner, researchers have included hyper-parameters in BMU (Behmanesh et al. 2015; Brynjarsdóttir and O'Hagan 2014; Gelman et al. 2013; Huang et al. 2017; Kennedy and O'Hagan 2001). However, inclusion of hyper-parameters makes the task of structural identification computationally more expensive and leads to problems of unidentifiability (Kuok and Yuen 2016). Often, hyper-parameter values are assumed to be invariate over the structure. Since model bias and other systematic uncertainties come from many sources, this is rarely the case for civil infrastructure.

To address challenges related to structural identification, Goulet and Smith (2013b) developed a multi-model probabilistic methodology for structural identification, called as error-domain model falsification (EDMF). This methodology, based on the philosophy of falsification by Popper (1959), has been successfully applied for interpretation of civil infrastructure measurement data. Using EDMF, enhanced predictions of reserve capacity related to remaining fatigue life (Pai et al. 2018; Pasquier et al. 2014), ultimate capacity (Proverbio et al. 2018c) and serviceability (Cao et al. 2020) have been made.

While many researchers have utilised data to enhance asset-management decision making, a challenge that has not been addressed is validation of structural-identification solutions. Without sufficient validation of identification solutions, predictions made using updated models may lead to non-conservative asset management. Pai et al. (2019) and Proverbio et al. (2018a) suggested the use of leave-one-out cross-validation to assess accuracy of structural identification solutions. While such validation may be sufficient for comparing data-interpretation methodologies, solutions are not necessarily accurate for making predictions outside the domain of the data (extrapolation).

In this paper, assessment of validation using information entropy is presented. Structural identification of a full-scale steel-concrete composite bridge using three data-interpretation methodologies is carried out using cross-validation strategies. Assessment of data used for validation is performed using joint entropy. If data utilised for validation contains exclusive information, *i.e.*, information that is not included in identification, then validation is appropriate for making predictions to support asset management decision-making. Once structural identification solutions are validated, an accurate estimation of the reserve capacity of the bridge with respect to remaining fatigue-life (RFL) becomes possible.

In addition to the contribution described above, a modified BMU methodology is presented. This methodology has already been shown to be numerically equivalent to EDMF (Pai et al. 2018, 2019; Pai and Smith 2017; Reuland et al. 2017). In this paper, the analytical equivalence of this new implementation of BMU and EDMF is presented.

2. DATA-INTERPRETATION METHODOLOGIES

In this section, three data-interpretation methodologies are described. These methodologies require various assumptions related to the uncertainties affecting the inverse problem of structural identification. Depending upon the validity of the assumptions made, the solutions obtained using these methodologies may be either accurate or inaccurate for further use to support the extrapolations that are part of asset-management decision making.

2.1 Error-domain model falsification

Error-domain model falsification (EDMF) is a model-based probabilistic data-interpretation methodology proposed by Goulet and Smith (2013b) that builds on more than a decade of research,

including over ten full-scale case studies (Smith 2016). This methodology is based on the assertion by Karl Popper (Popper 1959) that data can be used to falsify (reject) models than validate them.

In EDMF, models instances with predictions that are incompatible with observations (data) are rejected. Model instances include the physics-based model with specific input values for model parameters. In EDMF, these model parameters are quantified as random variables. The probability distribution of these random variables is estimated using engineering knowledge (Goulet and Smith 2013; Pasquier and Smith 2015). The Initial model set (IMS) includes various possible model instances (physics-based model with samples of model-parameters values).

For example, beam depth and modulus of elasticity of a beam are model parameters involved in a model for beam deflection. In this example, these parameters can be quantified as random variables and samples of these parameters serve as input to a physics-based model for simulating beam deflection. Combinations of samples drawn of these parameters and provided as input to the physics-based model form instances of the IMS.

The task of selecting appropriate parameters to sample and form the IMS is part of model-class selection. The task of model-class selection involves selecting a model from competing choices and selection of model parameters that are identifiable using monitoring data (Ljung 2010). Traditionally, the selection of model parameters for identification (and to form the IMS) is performed using various forms of sensitivity analysis (Van Buren et al. 2013, 2015; Friedman 1991; Matos et al. 2016). Recently, Pai et al. (2021) have suggested using machine learning methods to develop a trade-off curve that provides engineers with guidance in selecting a suitable model class for structural identification.

In EDMF, when a model in the IMS provides predictions that are incompatible with observations (measurements) it is falsified (rejected). Model instances that are not falsified after testing against all measurements form the candidate model set (CMS). These model instances are parameter-value combinations that, when provided as input to a physics-based model, provide predictions that are compatible with observations (measurements).

Let a structure be represented by a physics-based model, $\boldsymbol{g}(\cdot)$ and the modelling uncertainty associated be $\epsilon_{\mathrm{mod},i}$. Modelling uncertainty arises from assumptions and choices made during development of the physics-based model. Typical approximations that are involved are modelling of the boundary conditions, loading conditions and material behavior. These approximations may differ between models and are made in to accommodate a lack of knowledge or to simplify model development and thus reduce computational costs of performing simulations.

Quantification of modelling uncertainty associated with a physics-based model is a challenging and knowledge-intensive task. Simplifications and choices made during model development may be unique to the model developed. Therefore, the engineer developing the model is an important source of knowledge to quantify modelling uncertainties (Brynjarsdóttir and O'Hagan 2014). With engineering knowledge, bounds of modelling uncertainty sources may be determined; other information such as variance is rarely available. With bounds as the only available information about uncertainties, uniform distributions are the most appropriate choice of probability distribution for uncertainty quantification. Such a choice also satisfies the principle of maximum entropy (Jaynes 1957). With more information related to some modelling assumptions, such as experimentally evaluated probabilistic material models, more precise uncertainty quantification may be possible. However, such uncertainties rarely dominate structural identification and subsequent decision making.

Let measurements recorded on the structure during a monitoring exercise be $\boldsymbol{y}$. Let the number of measurements recorded be m and uncertainty associated with measurement at a location i be $\epsilon_{\text{meas},i}$. For an instance of model parameters, $\boldsymbol{\theta}$, provided as input to the physics-based model, let predictions at measurement locations be, $\boldsymbol{g(\theta)}$. Let Q_i be the real response of the structure at location i, which is related to measured and model-predicted value, as shown in Eq. (1).

$$Q_i = g_i(\theta) + \epsilon_{\text{mod},\,i} = \; y_i + \epsilon_{\text{meas},\,i} \tag{1}$$

Rearranging Eq. (1), provides Eq. (2) shown below, which relates residuals between model predictions and measurements with combination of measurement and modelling uncertainties at measurement locations.

$$g_i(\theta) - \; y_i = \; \epsilon_{\text{meas},\,i} - \; \epsilon_{\text{mod},\,i} \tag{2}$$

For an instance of model parameters, $\boldsymbol{\theta}$, the model predictions at sensor locations, $\boldsymbol{g(\theta)}$, are assessed for compatibility with measurements, $\boldsymbol{y}$, in EDMF. This assessment of compatibility is carried out on the basis of Eq. (3).

$$T_{\text{low},i} \leq g_i(\theta) - y_i \leq T_{\text{high},i} \qquad\qquad i \in [1,\ldots,m] \tag{3}$$

In Eq. (3), $g_i(\theta)$-y_i, is the residual between measurement and model predictions at a measurement location, i. $T_{\text{low},i}$ and $T_{\text{high},i}$ are compatibility thresholds calculated for measurement location i. These compatibility thresholds are calculated based on the modelling and measurement uncertainties that are affecting the task of structural identification, as shown in Eq. (2).

Let ϵ_i be the combined uncertainty at a measurement location i. This combined uncertainty is calculated by combining modelling uncertainty, $\epsilon_{\text{mod},i}$, with measurement uncertainty, $\epsilon_{\text{meas},i}$ using Monte Carlo sampling (Cox and Siebert 2006). Other sampling methods such as Latin hypercube

sampling and stratified sampling (McKay et al. 1979) may be used to combine uncertainties from multiple sources to obtain a combined distribution of uncertainty. To obtain the combined uncertainty PDF, random samples from modelling and measurement uncertainties are generated and these samples are combined together ($\epsilon_{meas,i}$ - $\epsilon_{mod,i}$). Using this combined uncertainty at a measurement location *i*, thresholds for falsification, $T_{low,i}$ and $T_{high,i}$, are calculated using Eq. (4).

$$\varphi^{1/m} = \int_{T_{low,i}}^{T_{high,i}} f(\varepsilon_i) \quad d\varepsilon_i \tag{4}$$

In Eq. (4), $f(\varepsilon_i)$ is the probability distribution function (PDF) of combined uncertainty at measurement location *i* and φ is the target reliability of identification. In Eq. (4), $\varphi \in [0,1]$ is the desired target reliability of identification (Goulet and Smith 2013). The target reliability of identification is a user-defined metric and sets the minimum required probability (level of confidence) that the ground truth (θ^*) is included in the set of solutions identified using EDMF.

While Eq.4 has an infinite number of solutions, the thresholds, $T_{high,i}$ and $T_{low,i}$, are computed as the ones that provide the shortest interval. Calculation of $T_{high,i}$ and $T_{low,i}$ may involve numerical errors directly related to the discretization (sampling) of the combined uncertainty PDF, $f(\varepsilon_i)$. This numerical error is lower when more samples are generated with random sampling to approximate the combined uncertainty PDF. However, these numerical precision errors are significantly smaller than errors from modelling sources ($\epsilon_{mod,i}$). In Eq. (4), the term *1/m* is the Sidak correction (Sidak 1967), which accounts for *m* independent measurements used in identification of model parameters.

If predictions for a model instance, θ_i, does not satisfy Eq. (3) for even one measurement location, then that model instance is falsified. All falsified model instances compose the falsified model set (FMS) (Goulet 2012; Goulet et al. 2010; Goulet and Smith 2013) as shown in Eq. (5).

$$\boldsymbol{\Omega}'' = \boldsymbol{\theta} \in \Omega \quad \forall i: \quad g_i(\theta) - y_i \quad \notin \quad \left[T_{\text{low},i}, T_{\text{high},i}\right] \tag{5}$$

Falsified model instances are assigned a probability of 0. The remaining parameter instances from the IMS, $\boldsymbol{\Omega}$, whose responses for all measurement locations lie within the thresholds, *i.e.*, they satisfy Eq. (5), form the CMS. The probability densities attributed to CMS and FMS are shown in Eq.(6).

$$p(\theta) = \begin{cases} 0 & \boldsymbol{\theta} \in \boldsymbol{\Omega}'' \\ \dfrac{1}{\int_{d\theta} \boldsymbol{\theta}} & \boldsymbol{\theta} \notin \boldsymbol{\Omega}'' \end{cases} \tag{6}$$

Due to a lack of knowledge of uncertainties, no model instance is assumed to be more likely than another in the CMS. Consequently, all model instances in the CMS are assumed to have a uniform probability density. As the knowledge of uncertainties is not known completely, the exact probability of one model instance being more likely than the other is also not known accurately. This assumption is conservative and accurate under the assumed uncertainty conditions. This assumption is also compatible with the accuracy of engineering knowledge that is available. It is important to ensure that the methodologies and representations do not provide a level of detail that cannot be warranted by the quality of input knowledge. Candidate models are used for making further predictions using the physics-based model (Pasquier and Smith 2015).

EDMF, when compared with BMU and residual minimization, has been shown to provide more accurate identification (Goulet and Smith 2013) and prediction (Pasquier and Smith 2015) than the more traditional methods that are described in Sections 2.2 and 2.3. EDMF is more accurate due to its robustness to correlation assumptions and explicit estimation of model bias based on engineering heuristics (Goulet and Smith 2013; Pasquier and Smith 2015).

2.2 Residual minimization

Residual minimization, also called model updating, model calibration and parameter estimation, originated from the work of Gauss and Legendre in the 19th century (Sorenson 1970). In residual minimization, a structural model is calibrated by determining model parameter values that minimize the error between model prediction and measurements. A typical objective function for residual minimization is shown in Eq. (7).

$$\hat{\theta} = \underset{\theta}{\operatorname{argmin}} \sum_{i=1}^{m} \left(\frac{g_i(\theta) - y_i}{y_i} \right)^2 \quad \textbf{(7)}$$

In Eq. (7), $\hat{\theta}$ is the optimum model parameter set obtained by minimising the sum of normalized square residual between model response, $g_i(\theta)$, and measurement, y_i, for all measurement locations, *i.e.*, $\forall\, i \in [1,\ldots m]$.

Residual minimization requires the assumption that the difference between model predictions and measurements is governed by the choice of parameter values (Mottershead et al. 2011). This inherently implies that model bias in civil infrastructure that is caused by application of safe design models is not taken into account. Moreover, this also requires the assumption that the uncertainties associated with each residual are independent and have zero means. The presence of systematic bias may lead to the assumption of independence not being fulfilled (Jiang and Mahadevan 2008; McFarland and Mahadevan 2008; Rebba and Mahadevan 2006). When these assumptions are not appropriate, residual minimization may not provide accurate identification (Beven 2000). Any model is intrinsically imperfect due to parameter-value compensation and ill-posed nature of structural identification task (Atamturktur et al. 2015; Beck 2010; Goulet and Smith 2013; Moon et al. 2013; Neumann and Gujer 2008). However, the simplicity of this methodology has made it

popular for use in structural (Brownjohn et al. 2001, 2003; Chen et al. 2014; Feng and Feng 2015; Mosavi et al. 2014; Sanayei et al. 2015) and geotechnical (Hashemi and Rahmani 2018; Levasseur et al. 2008; Rechea et al. 2008; Zhang et al. 2013) applications, among many others.

While identification with residual minimization may occasionally be accurate, prognosis and predictions with models updated using residual minimization are limited to the domain of data used for calibration (Schwer 2007). Therefore, calibrated model-parameter values may be suitable for interpolation predictions (within the domain of data used for calibration) (Schwer 2007). They are, however, not suitable for extrapolation (predictions outside the domain of data used for calibration) (Beven 2000; Mottershead et al. 2011).

2.3 Bayesian model updating

BMU is a data-interpretation methodology that is based on Bayes' theorem (Bayes 1763). Use of BMU for structural identification was popularized in late 1990's (Alvin 1997; Beck and Katafygiotis 1998; Katafygiotis and Beck 1998). In BMU, prior information of model parameters, $p(\theta)$, is conditionally updated using a likelihood function, $p(y|\theta)$, to obtain a posterior distribution of model parameters, $p(\theta|y)$, as shown in Eq.(8).

$$p(\theta|y) = \frac{p(\theta) \cdot p(y|\theta)}{p(y)} \quad \textbf{(8)}$$

In Eq.(8), $p(y)$ is a normalization constant. The likelihood function, $p(y|\theta)$ is the probability of observing the measurement data, y, given a specific set of model-parameter values, θ. The likelihood function leverages information gained from measurements to create a mapping between residuals (difference between model predictions and measurements) in error domain, Ξ, and the parameter domain, Ω (Goulet and Smith 2013).

2.3.1 Traditional Bayesian model updating

Traditionally, BMU has been carried out using a L_2-norm-based Gaussian PDF, as a likelihood function, as shown in Eq.(9).

$$p(y|\theta) \propto \text{constant} \cdot \; e^{\left[-\frac{1}{2}(\boldsymbol{g}(\boldsymbol{\theta})-\boldsymbol{y})^{\mathrm{T}}\Sigma^{-1}(\boldsymbol{g}(\boldsymbol{\theta})-\boldsymbol{y})\right]} \quad \textbf{(9)}$$

In Eq. (9), $\boldsymbol{g(\theta)} - \boldsymbol{y}$, is the residual between model response, $\boldsymbol{g(\theta)}$, and measurements, $\boldsymbol{y}$ and Σ is a covariance matrix that consists of variances and correlation coefficients of uncertainties for each measured location.

In this traditional application of BMU, uncertainties at measurement locations are assumed to be defined by independent zero-mean Gaussian distributions (Beck et al. 2001; Ching and Beck 2004; Katafygiotis et al. 1998; Muto and Beck 2008; Yuen et al. 2006). In addition, the variance in uncertainty, σ^2 is assumed to be the same for all measurement locations, which leads the covariance matrix to be a diagonal matrix, with all non-zero terms being equal. However, the dubious assumptions of a Gaussian distribution for model uncertainty (Tarantola 2005) and uncorrelated error (Simoen et al. 2013) are rarely satisfied in civil-engineering systems and this leads to wrong updated probability distributions (Goulet and Smith 2013; Pasquier and Smith 2015).

2.3.2 Modified Bayesian model updating

To alleviate shortcomings of traditional BMU, a box-car likelihood function is presented in this section. This likelihood function is more robust to incomplete knowledge of uncertainties and correlations compared with traditional assumptions of normality and independence. Moreover, model updating with a box-car-shaped likelihood function has been shown numerically to provide results that are compatible with those obtained using EDMF (Pai et al. 2018, 2019; Pai and Smith

2017; Reuland et al. 2017). In this section, this compatibility is demonstrated analytically, which complements the numerical compatibility that has been observed previously.

The modified L_∞ norm-based Gaussian likelihood function is developed using the thresholds (T_{low} and T_{high}) determined for EDMF. The objective of this new likelihood function is to update knowledge of structural behaviour in the presence of biased, non-Gaussian sources of uncertainty with unknown correlations. A generalized Gaussian distribution is defined as shown in Eq.(10).

$$p(\boldsymbol{x}|\boldsymbol{\theta},\kappa) = \frac{\kappa^{1-q/\kappa}}{2\boldsymbol{\sigma}_{\boldsymbol{\kappa}}\Gamma\left(1/\kappa\right)} e^{\kappa\left[\frac{|\boldsymbol{x}-\boldsymbol{\mu}_{\boldsymbol{x}}|}{\boldsymbol{\sigma}_{\boldsymbol{\kappa}}}\right]^{\kappa}} \quad \textbf{(10)}$$

Eq. (10) is valid for a random variable x, based on κ-norm with mean, $\boldsymbol{\mu}_{\boldsymbol{x}}$, and standard deviation, $\boldsymbol{\sigma}_{\boldsymbol{\kappa}}$. As $\kappa \to \infty$, $p(x|\theta,\kappa)$ tends to a box-car shape. The likelihood function, $p(y|\theta)$, for infinity norm is given in Eq. (11)

$$p(\boldsymbol{y}|\boldsymbol{\theta}) = \begin{cases} 1/2\boldsymbol{\sigma}_{\infty} & \text{for } \boldsymbol{\mu}_{\boldsymbol{x}} - \boldsymbol{\sigma}_{\infty} \le \boldsymbol{g}(\boldsymbol{\theta}) - \boldsymbol{y} \le \boldsymbol{\mu}_{\boldsymbol{x}} + \boldsymbol{\sigma}_{\infty} \\ 0 & \text{otherwise} \end{cases} \quad \textbf{(11)}$$

In Eq. (11), parameters of the likelihood function $\boldsymbol{\mu}_{\boldsymbol{x}}$ and $\boldsymbol{\sigma}_{\boldsymbol{\kappa}}$, are determined using Eq. (12) and Eq.(13). The random variable x represents the combined uncertainty associated with the structural identification task, ϵ_i.

$$\boldsymbol{\mu}_{\boldsymbol{x}} = \frac{\boldsymbol{T}_{\boldsymbol{high}} + \boldsymbol{T}_{\boldsymbol{low}}}{\mathbf{2}} \quad \textbf{(12)}$$

$$\boldsymbol{\sigma}_{\infty} = \boldsymbol{T}_{\boldsymbol{high}} - \boldsymbol{\mu}_{\boldsymbol{x}} \quad \textbf{(13)}$$

In using Eq. (12) and Eq.(13), $\boldsymbol{T}_{\mathbf{low}}$ and $\boldsymbol{T}_{\mathbf{high}}$ are the thresholds computed for EDMF using Eq. (4) for a target reliability of identification, ϕ (assumed to be equal to 0.95 in this paper). The likelihood

function is developed with no inherent assumptions related to the distribution and bias of combined uncertainty at measurement locations.

Figure 1 shows a graph of the likelihood function developed based on the EDMF thresholds for application of modified BMU on a full-scale bridge that is explained later on in this paper. In the uncertainty (error) domain, the likelihood function and the thresholds for EDMF define a similar region as shown in Figure 1.

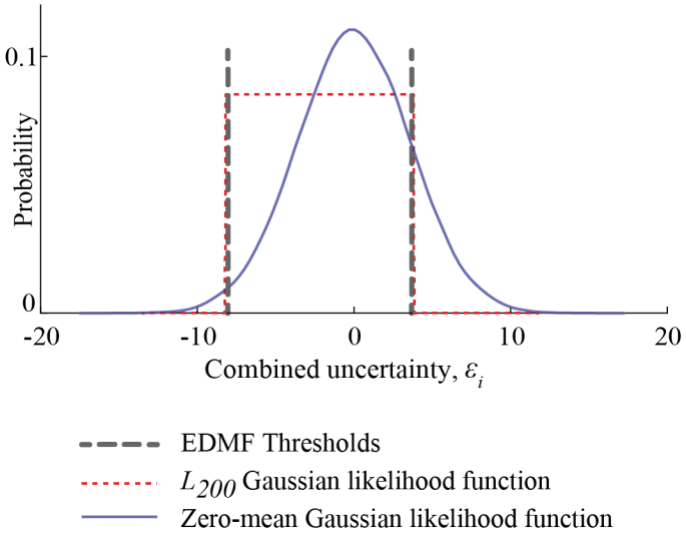

Figure 1 Comparison between L_∞-norm Gaussian likelihood function and EDMF thresholds

In Figure 1, marginal PDF of uncertainty at a measurement location, i estimated as a L_{200}-norm Gaussian likelihood function (approximation of a L_∞-norm Gaussian function) is shown, which is calculated using Eq. (10(11) with shape factor, $\kappa = 200$. This PDF of uncertainty has bounds similar to the EDMF thresholds, T_{low} and T_{high}, which are calculated using the combined uncertainty at a measurement location i using Eq. (4). Figure 1 also shows a comparison of traditional bell-shaped L_2-norm-based Gaussian likelihood function (see Eq. (9) with an L_{200}-norm-based Gaussian likelihood function estimation of uncertainty at measurement location i. The modified likelihood

function explicitly accounts for model bias and makes conservative estimations of uncertainty (Jaynes 1957) at a measurement location with incomplete information (thresholds or bounds).

Let $\boldsymbol{g(\theta)}$ be the model of a structure with parameters $\boldsymbol{\theta}$. In the absence of complete information related to model parameters, the prior PDF of these parameters, $p(\boldsymbol{\theta})$, can be assumed to be uninformative, with a uniform density p. The probability distribution of these parameters can be updated using Eq.(8) using information from measurements $\boldsymbol{y}$. Eq. (14) provides the posterior PDF, $p(\boldsymbol{\theta}|\boldsymbol{y})$, of model parameters, $\boldsymbol{\theta}$, using the L_∞-norm-based Gaussian likelihood function as defined in Eq.(11).

$$p(\boldsymbol{\theta}|\boldsymbol{y}) = \begin{cases} \dfrac{p \cdot 1/2\boldsymbol{\sigma}_\infty}{p(\boldsymbol{y})}, & \text{for } \boldsymbol{\mu_x} - \boldsymbol{\sigma}_\infty \le \boldsymbol{g}(\boldsymbol{\theta}) - \boldsymbol{y} \le \boldsymbol{\mu_x} + \boldsymbol{\sigma}_\infty \\ \mathbf{0}, & \text{otherwise} \end{cases} \quad \textbf{(14)}$$

Eq. (14) provides posterior PDF of model parameters based on the residual between model predictions, $\boldsymbol{g(\theta)}$ and measurements, $\boldsymbol{y}$. According to Eq.(14), the posterior probability distribution for model parameters $\boldsymbol{\theta}$, which satisfy the condition, $\boldsymbol{\mu_x - \sigma_\infty \le g(\theta) - y \le \mu_x + \sigma_\infty}$, are distributed with density $p/2\boldsymbol{\sigma}_\infty \cdot p(y)$. Let this region of model parameters with non-zero probability be denoted by $\boldsymbol{\Omega_{mBMU}}$. Substituting Eq.(12) and Eq.(13) into the condition defining the region $\boldsymbol{\Omega_{mBMU}}$, the new condition for this region based on the EDMF thresholds is $\boldsymbol{\theta} \in \boldsymbol{\Omega_{mBMU}}$ for $\boldsymbol{g}(\boldsymbol{\theta}) - \boldsymbol{y} \in [\boldsymbol{T_{low}}, \boldsymbol{T_{high}}]$. Comparing this with Eq.(6), the non-zero probability region obtained using EDMF (CMS) is the same as $\boldsymbol{\Omega_{mBMU}}$, which is obtained using BMU with a box-car likelihood function.

The space defined by $\boldsymbol{\Omega_{mBMU}}$ is equivalent to the space CMS defined for EDMF using Eq. (6). Since the posterior probability density under both sets of parameter space is defined as a constant (see Equations (6 and (14) and since the integral of the posterior PDFs for both sets have to be equal to 1, the posterior densities of the updated parameter spaces are equal.

EDMF is more robust to assumptions about correlations between uncertainties at various sensor locations than implementations using Gaussian distributions (Goulet and Smith 2013). This has been demonstrated to be an important condition to obtain accurate structural identification (Simoen et al. 2013). Furthermore, changes in values of systematic uncertainties, such as boundary conditions, can change correlations between uncertainties (Goulet and Smith 2013). BMU with L_∞-norm-based Gaussian likelihood function provides results that are equivalent to EDMF and are robust to changes in correlations between uncertainties at sensor-location pairs, as shown in Figure 2.

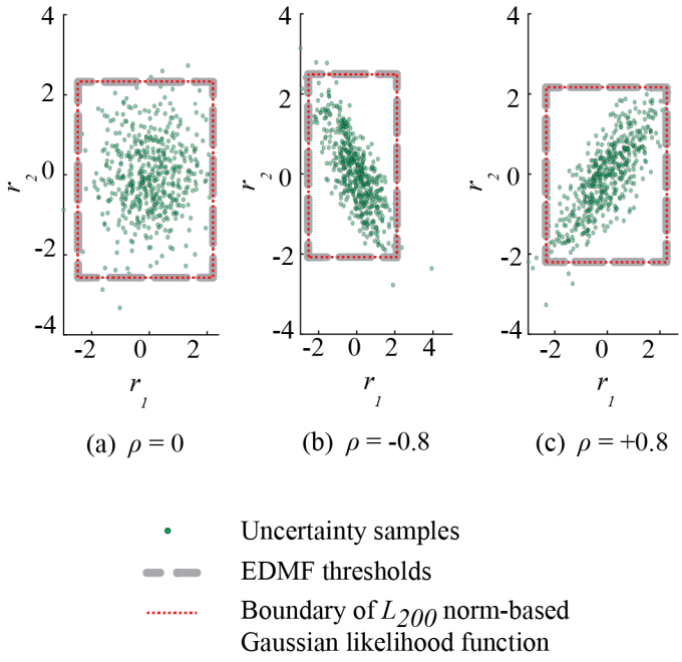

Figure 2 Robustness to changing correlations

Figure 2 shows samples of error between model response and measurement, $\boldsymbol{r_1}$ and $\boldsymbol{r_2}$, for two measurement locations assuming three different correlation values. In Figure 2 (a), the correlation between samples of $\boldsymbol{r_1}$ and $\boldsymbol{r_2}$ is zero, *i.e.*, $\boldsymbol{r_1}$ and $\boldsymbol{r_2}$ are independent. As shown in the figure, the threshold bounds and high-density region of the L_∞-norm-based Gaussian likelihood function

336 overlap. The bounded region includes at least 95 percentile of the error samples. In Figure 2 (b)
337 and (c), correlations between the error samples are -0.8 and 0.8, respectively. For both of these
338 scenarios, the bounded region includes at least 95^{th} percentile of the error samples. Therefore,
339 BMU with the L_∞-norm-based Gaussian likelihood function is robust to changes in correlations
340 and provides robust results in a similar way to EDMF.

341 Application of EDMF has practical advantages compared with this modified implementation of
342 BMU. Development of the likelihood function, which involves conditional probabilities, is more
343 complex and is less compatible with typical engineering knowledge and practise. EDMF has a
344 simpler and easy-to-understand updating criteria using threshold bounds. Additionally, grid
345 sampling with EDMF is analogous to typical trial and error methods used in practise. BMU
346 typically involves adaptive sampling methods such as Markov Chain Monte Carlo (MCMC)
347 (Tanner 2012). Moreover, the L_∞-norm-based Gaussian likelihood function is approximated using
348 a L_{200}-norm-based Gaussian likelihood function for implementation as shown in Figure 1. Such
349 approximations lead to differences between solutions obtained with EDMF and modified BMU.
350 A detailed evaluation of practical advantages of EDMF compared with this modified Bayesian
351 implementation is provided by Pai et al. (2019).

352 **3. VALIDATING STRUCTURAL IDENTIFICATION**

353 Validation of structural identification of full-scale case studies is a challenging task. In full-scale
354 case studies, the true parameter values (ground truth) is not known. Methods for cross-validation
355 provide indications of the accuracy of structural identification solutions without knowledge of the
356 ground truth. In the next section, two methods of cross-validation for structural identification are
357 presented.

3.1 Validation

EDMF, compared with traditional BMU and residual minimization, has been shown to provide accurate model updating for theoretical cases using simulated measurements (Goulet and Smith 2013; Pasquier and Smith 2015). In these theoretical comparisons, the ground truth values are known. For assessment of accuracy of full-scale structures, data-driven methods can potentially provide quantitative validation.

Comparisons of EDMF with traditional BMU and residual minimization have been made for full-scale case studies using leave-one-out cross-validation (Pai et al. 2019) and hold-out cross-validation (Pai et al. 2018). In these comparisons, one or more measurements (data points) are excluded during identification. Subsequent to identification, the updated parameter values are used to predict response at measurement locations that were excluded. If the predicted response is similar to the measurement value, then structural identification is assumed to be validated (Vernay et al. 2018).

EDMF and modified BMU provided updated parameter distributions, which when used to predict response (with modelling uncertainties) provide prediction distributions that may be assumed to be uniformly distributed. Bounds of these updated prediction distributions must include the measured value left out from structural identification for solutions obtained to be accurate. If the updated prediction bounds do not include the measured value, then structural identification is inaccurate, as shown in Eq. (15).

$$\text{Accuracy, } \Psi_i = \begin{cases} 1 & \text{for } y_i \in \left[\min\left[g_i(\theta"), \max[g_i(\theta")]\right]\right] \\ 0 & \text{for } y_i \notin \left[\min\left[g_i(\theta"), \max[g_i(\theta")]\right]\right] \end{cases} \quad \textbf{(15)}$$

In Eq. (15), Ψ_i is a binary variable with value equal to 1 for accurate structural identification and 0 for inaccurate structural identification at a measurement data point *i*, which is held out for validation. In the equation, ***θ"***, are instances from updated model parameter distributions obtained using EDMF and modified BMU.

Predictions with updated model-parameter distributions obtained using traditional BMU leads to informed (not uniform) prediction distributions. To assess accuracy, measurement recorded may either be compared with the median value or with the 95th percentile bounds of the updated prediction distribution. In this paper, traditional BMU is assessed to provide accurate structural identification when the measurement value lies within the 95th percentile bounds of the updated prediction distribution as shown in Eq. (16).

$$\text{Accuracy}, \Psi_i = \begin{cases} 1 & \text{for } y_i \in \left[P_{95}\left(g_i(\theta")\right)\right] \\ 0 & \text{for } y_i \notin \left[P_{95}\left(g_i(\theta")\right)\right] \end{cases} \quad \textbf{(16)}$$

In Eq. (16), P_{95} are the 95th percentile bounds of the updated prediction distribution, $g_i(\boldsymbol{\theta"})$, at a measurement point *i*. Similarly, residual minimization is taken to provide accurate identification when the updated prediction lies close to the measurement value (within 95th percentile bounds of measurement uncertainty, no modelling uncertainty considered in residual minimization), as shown in Eq. (17).

$$\text{Accuracy}, \Psi_i = \begin{cases} 1 & \text{for } g_i(\hat{\theta}) \in \left[P_{95}\left(y_i + \epsilon_{\text{meas},i}\right)\right] \\ 0 & \text{for } g_i(\hat{\theta}) \notin \left[P_{95}\left(y_i + \epsilon_{\text{meas},i}\right)\right] \end{cases} \quad \textbf{(17)}$$

In Eq. (17), y_i, is a measurement held out from structural identification and $\epsilon_{\text{meas},i}$ is the measurement uncertainty associated with the recording. P_{95} are the 95th percentile bounds of the

measured value including measurement uncertainty. $\boldsymbol{g_i}(\hat{\theta})$ is the prediction at measurement point, *i*, with updated optimal parameter instance, $\hat{\theta}$.

Equations, (15), (16) and (17), provide conditions to determine whether updated predictions at locations of measurements not included for structural identification are accurate. However, in data-driven methods for cross-validation (Golub et al. 1979; Kohavi and others 1995) such as leave-one-out and hold-out cross-validation (Hong and Wan 2011), the data points left out may or may not contain new information. If information contained in the validation dataset is not exclusive, then validation with redundant data is not suitable for assessment of accuracy.

No research so far has been carried out to assess exclusivity of information in validation data and suitability of validated solutions for making further predictions to support asset management decision-making. In the next section, the concept of joint entropy and information gain is introduced. This concept helps assess whether data used for validation contains exclusive information.

3.2 Joint entropy and mutual information

Information entropy was introduced as a sensor-placement objective function for system identification by Papadimitriou et al. (2000). Information entropy is a measure of disorder in predictions obtained at a sensor location due to changes in model-parameter values (Robert-Nicoud et al. 2005). High values for information entropy indicate higher disorder in model-instance predictions, and this makes these locations attractive for sensor placement. Consequently, response at these locations (model predictions) is more sensitive to variations in structural behaviour (parameter values) than at locations having low entropy values. Therefore,

measurements at high entropy locations have more potential to improve structural identification than at low-entropy locations.

Within any system, measurements are typically correlated, leading to redundancy in information gain. Papadopoulou et al. (2014) developed a joint entropy metric to assess information gain from measurements from multiple sensors, while accounting for redundancy.

Let H($g_{i,i+1}$) be the joint entropy of predictions at measurement locations i and i+1. Let $H(g_i)$ and H(g_{i+1}) be the information entropy at these measurement locations. Joint entropy, H($g_{i,i+1}$) is less than or equal to the sum of individual information entropies, $H(g_i)$ and $H(g_{i+1})$ due to redundancy in information gain, I($g_{i,i+1}$). This redundancy in information, I($g_{i,i+1}$), can be calculated using Eq. (18).

$$H(g_{i,i+1}) = H(g_i) + H(g_{i+1}) - I(g_{i,i+1}) \quad \textbf{(18)}$$

Eq. (18) can be re-ordered to calculated the mutual (redundant) information, I($g_{i,i+1}$), between measurements at two sensor locations. Consequently, Eq. (18) may be extended to sets of data from multiple sensors as shown in Eq.(19).

$$H(g_{\mathrm{A,B}}) = H(g_{\mathrm{A}}) + H(g_{\mathrm{B}}) - I(g_{\mathrm{A,B}}) \quad \textbf{(19)}$$

In Eq. (19), A and B are two sets of measurement locations. $H(g_A)$ and $H(g_B)$ are the joint entropies for predictions at these two sets of locations. The total joint entropy including locations in sets A and B is $H(g_{A,B})$. The redundancy in information between these two sets of model-predictions data is $I(g_{A,B})$.

In Eq. (19), let A be a set of measurement locations, data (measurements) from which is used for structural identification (identification set). Similarly, let B be a set of measurement locations, data

(measurements) from which are held-out for validation after structural identification (validation set). Redundancy in information between data used for identification and validation, $I(g_{A,B})$, may be calculated using Eq. (19), as shown in Eq.**(**20).

$$I(g_{\mathrm{A,B}}) = H(g_{\mathrm{A}}) + H(g_{\mathrm{B}}) - H(g_{\mathrm{A,B}}) \quad \textbf{(20)}$$

Validation of structural identification is accurate when data used for validation provides new information regarding structural behaviour, which is not available in the data used for identification. This new information may be assessed using the metric of information entropy as shown in Eq. (19). Exclusive information in validation set B, E_B, which is not included in identification set A, is calculated as shown in Eq. (21).

$$E_B = H(g_B) - I(g_{A,B}) \quad \textbf{(21)}$$

In Eq. (21), the quantity $H(g_B)$ is the joint entropy of validation set B and $I(g_{A,B})$ is the redundancy in information between identification set A and validation set B. $I(g_{A,B})$ is calculated using Eq.**(**20).

Let *m* measurements be available for structural identification. In leave-one-out cross-validation, one measurement is held out from identification for validation. Structural identification is performed using *m*-1 measurements (identification set A). The measurement held out is the validation set B. The exclusive information available for validation using this one measurement is calculated using Eq. (21). As *m* measurements are available, *m* iterations of validation by leaving each sensor out can be carried out.

For holdout cross-validation, instead of only one measurement, let *h* measurements out of *m* be held out for validation. In this case, the identification set includes *m*-*h* measurements, which forms

452 the identification set A. The validation set B includes *h* measurements. The exclusive information
453 in set B, not available for identification in set A, is calculated using Eq. (21).

454 For both validation methods, data used for validation must include new and exclusive information
455 to be able to assess accuracy of structural identification. Low or negative values of exclusive
456 information, E_B, indicate either uninformative data, *i.e.*, low $H(g_B)$ or large redundancy in
457 information between identification and validation data *i.e.*, high $I(g_{A,B})$.

458 In the next section, the application of structural identification methodologies for evaluation of a
459 full-scale bridge case study is presented. The results of structural identification are assessed using
460 leave-one-out and hold out cross-validation methods. Subsequent to assessment of accuracy of
461 structural identification, fatigue life of the bridge at a critical detail is evaluated using updated
462 knowledge of structural behaviour acquired using measurements.

463 **4. POWDER MILL BRIDGE**

464 In this section, the three data-interpretation methodologies described previously have been applied
465 for structural identification of the Powder Mill Bridge (PMB) (Follen et al. 2014) shown in Figure
466 3. This bridge has also been called the Vernon Avenue Bridge (Sanayei et al. 2011). The PMB is
467 a steel-concrete bridge built over the Ware river in Barre, Massachusetts, USA. The bridge was
468 built in 2009 and connects the state highway with a depot road that services mainly truck traffic.

(a) Truck over PMB (b) Side view of PMB

Figure 3 Powder Mill Bridge (PMB) located in Massachusetts, USA.

Figure 4 shows a schematic drawing of the PMB. This bridge has three spans with a total length of 47 m. The bridge has a concrete deck, which is supported by six I-section steel girders as shown in the figure.

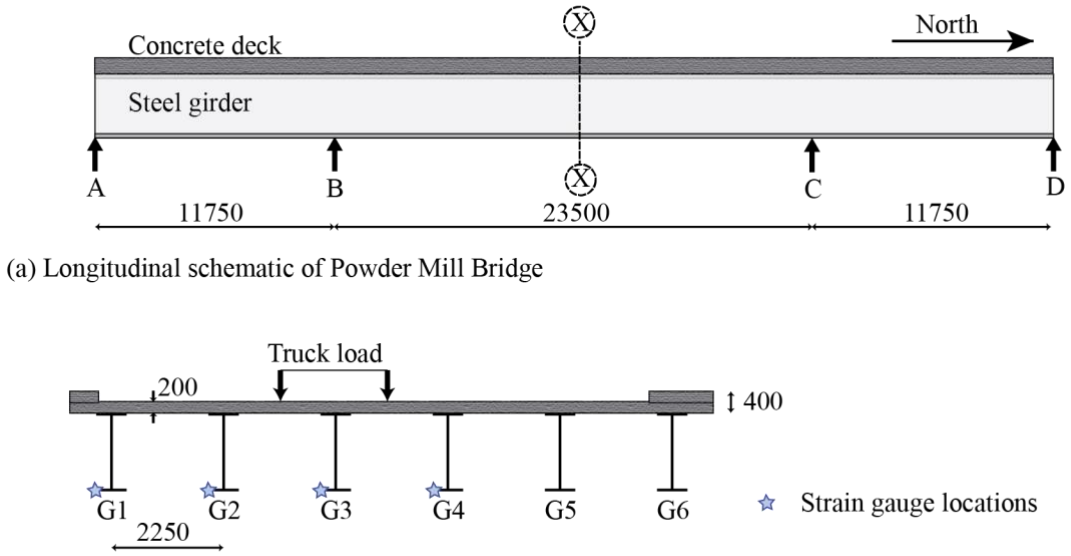

(a) Longitudinal schematic of Powder Mill Bridge

(b) Transverse schematic of Powder Mill Bridge at X-X

Figure 4 Schematic drawing of the Powder Mill Bridge

4.1 Load test and measurements

A load test was performed on the PMB. During the load test, a truck weighing 33 tonnes was driven across the bridge at a speed of 10 km/h to avoid dynamic amplification effects. The transverse alignment of the truck on the bridge is shown in Figure 4 (b). The response of the bridge to this truck loading was recorded using strain gauges. Strain gauges were placed on the lower flange of the steel girders as shown in Figure 4 (b). The placement of the gauges in plan view is shown in Figure 5. In total, 20 strain gauges recorded structural response during the load test.

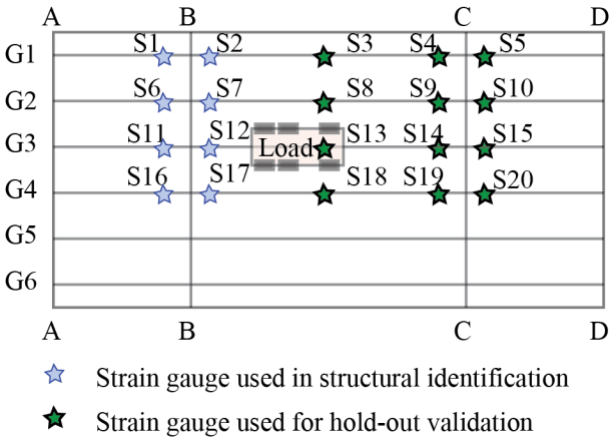

Figure 5 Location of 20 strain gauges installed on the bridge to record data during the load test. Data from 8 sensors is used for identification (and leave-one-out cross-validation). Data from remaining 12 sensors is used for hold-out cross-validation of structural identification.

Strain from 8 sensors, S1, S2, S6, S7, S11, S12, S16 and S17, shown in Figure 5 are used in this paper for structural identification of the PMB. Data from other sensors is held-out for cross-validation. The data utilised for structural identification corresponds to the point in time when movement of the truck leads maximum strain recorded in S13 (see Figure 5).

The objective of measuring this bridge is to update a FE model and enable better prediction of the remaining fatigue-life (RFL) of the bridge. A fatigue critical detail on the bridge that has been identified is a welded cover plate detail near support C at the bottom flange of girder G2 (see

Figure 5). In the next section, the development of a FE model of the bridge and estimation of uncertainties affecting the task of structural identification are described.

4.2 Model development and uncertainties

To interpret data recorded during the load test, a finite element (FE) model of the bridge has been developed in Ansys (APDL 2010). In the FE model, the concrete deck is modelled as a homogeneous slab using four-node SHELL182 elements (ANSYS 2012). The steel girders are modelled using SHELL182 elements.

The connection between the steel girders and concrete deck (in transversal and longitudinal directions) is modelled using zero-length spring elements (COMBIN14). The end supports of the bridge (support A and D) and intermediate supports (Support B and C) are modelled with zero-length spring elements (COMBIN14) with parameterized stiffness in longitudinal and vertical directions. Springs belonging to each support have been parameterized individually to account for any changes in structural behaviour between supports.

The footpath on the bridge and the railings also contribute to bridge structural behaviour (Sanayei et al. 2011). However, stiffness of the connection between the concrete deck and railings is not known. Thus, the deck slab thickness and thickness of the deck and railing at the edge of the bridge are parameterized in the FE model. Table 1 shows the parameters included in the FE model and the prior distributions assumed for these parameters based on engineering heuristics.

Table 1 Parametric sources of uncertainty in the model and their range

Index	Parameter	Variable	Range
1	Modulus of elasticity of concrete (GPa)	E_c	20-55
2	Modulus of elasticity of steel (GPa)	E_s	195-210
3	Thickness of deck slab (mm)	H_d	200-210
4	Height of concrete slab, sidewalk and railing (mm)	H_r	300-500
5	Deck-girder connection stiffness, transversal (log N/mm)	$K_{dg,x}$	2-6
6	Deck-girder connection stiffness, longitudinal (log N/mm)	$K_{dg,z}$	4-10
7	Vertical stiffness of abutment A (log N/mm)	$K_{1,y}$	4-7
8	Horizontal stiffness of abutment A (log N/mm)	$K_{1,z}$	2-5
9	Vertical stiffness of pier B (log N/mm)	$K_{2,y}$	4-7
10	Horizontal stiffness pier B (log N/mm)	$K_{2,z}$	2-5
11	Vertical stiffness of pier C (log N/mm)	$K_{3,y}$	4-7
12	Horizontal stiffness of pier C (log N/mm)	$K_{3,z}$	2-5
13	Vertical stiffness of abutment D (log N/mm)	$K_{4,y}$	4-7
14	Horizontal stiffness of abutment D (log N/mm)	$K_{4,z}$	2-5

Not all parameters included in the FE model influence structural behaviour significantly. Based on a sensitivity analysis, a model class is chosen for structural identification. The parameters included in the model class for structural identification are E_c, H_r, $K_{dg,x}$, $K_{2,y}$ and $K_{3,y}$. The prior distributions of these parameters are presented in Table 1.

Identification of the five parameters in the model class is carried out using three data-interpretation methodologies in this paper. The task of structural identification is computationally expensive, especially when it has to be repeated for three methodologies. To alleviate the computational load, the FE model has been replaced with a set of surrogate models. One simulation with a FE model takes a few minutes (approximately five minutes using an Intel(R) Xeon(R) CPU E5-2670 v3 @2.30GHz processor) while one simulation with surrogate models takes less than a second. The computational cost of using an FE models increases drastically when thousands of simulations have to be performed to search for solutions using the data-interpretation methodologies. Therefore, use of surrogate models successfully alleviates this computational cost.

The methodology adopted for development of the surrogate models is Gaussian process regression. One regression model each has been developed to replicate the FE model response at each sensor location. The surrogate models are trained and validated (hold-out) using data simulated using the FE model for various parameter-value combinations based on the model class for identification.

Updating the parameters requires assessment of uncertainties affecting the task of structural identification. Uncertainties are given in Table 2. Measurement uncertainty is estimated based on knowledge of sensors.

Load uncertainty includes uncertainty from the magnitude of the truck load and uncertainty in its position on the bridge. This uncertainty is quantified by varying the position of the truck and its load within reasonable limits based on engineering heuristics. The affect of this variability on the model response at sensor locations is used to quantify the load uncertainty related to magnitude and position.

Model bias is estimated based on an engineering understanding of assumptions made during model development. Assumptions involved in development of the model include the choice of finite element, modelling of the boundary conditions as springs and homogeneous modelling of the concrete slab. While no objective quantification of these assumptions is possible (Goulet et al. 2013), model bias, as tabulated in Table 2, is largely based on the engineering knowledge that is available.

Surrogate model uncertainty is the error between surrogate model predictions and predictions obtained using the FE model. This uncertainty is estimated based on hold-out cross-validation of the surrogate models.

Table 2 Uncertainty sources and their distribution (%). Uncertainty from measurements is quantified as normal distributions (N) and uncertainty from other sources are quantified as uniform probability distributions (U).

Source	Distribution
Measurement	N (0, 5)
Load	U (-5, 5)
Model bias	U (-15, 5)
Surrogate model uncertainty	U(-1,1)

Apart from the uncertainties listed in Table 2, there is uncertainty from parameters in the FE model that have not been included in the model class for identification. This parameter uncertainty is calculated using the FE model and is estimated to be uniformly distributed with bounds -15% and + 5% at all sensor locations.

Combining uncertainties from Table 2 with parameter uncertainty (-15% to +5%), structural identification of the PMB is carried out. These uncertainties are combined together to obtain the combined uncertainty PDF as explained in Section 2.1. This combined uncertainty is utilised to calculate the falsification thresholds for EDMF using Eq.(4) and the likelihood functions for traditional and modified BMU using Eq.(9) and Eq. (10).

4.3 Structural identification

Structural identification for the PMB using data from eight strain gauges has been carried out using EDMF, traditional BMU, modified BMU and residual minimization. In Figure 6, marginal posterior PDFs of model parameters obtained after structural identification using EDMF, traditional BMU, modified BMU and residual minimization are presented.

In Figure 6, initial model instances identified as compatible with measurements using EDMF (CMS) and modified BMU ($\boldsymbol{\Omega_{mBMU}}$) are similar. This equivalency in identification between EDMF and modified BMU has been demonstrated analytically in Section 2.3.2. However, in

571 Figure 6, the bounds of parameters E_c and $K_{2,y}$ identified using EDMF and modified BMU are
572 similar but not the same due to variations in the sampling methodologies adopted and
573 approximation of the box-car likelihood function using a L_{200}-norm-based Gaussian likelihood
574 function (instead of a L_∞-norm-based Gaussian likelihood function). Also, EDMF utilizes an
575 engineering compatible grid sampling (Pai et al. 2019), while modified BMU is carried out using
576 MCMC sampling (Tanner 2012). Due to these differences in practical application of EDMF and
577 modified BMU, results obtained with these methodologies may differ.

578 Updated PDFs of model parameters obtained using traditional BMU and the optimal parameter
579 values obtained using residual minimization are shown in Figure 6. While Figure 6 shows the
580 updated parameter distributions, it does not provide any information regarding accuracy of the
581 updated parameter distributions. In the next section, multiple cross-validations have been carried
582 out to assess accuracy of structural identification solutions obtained.

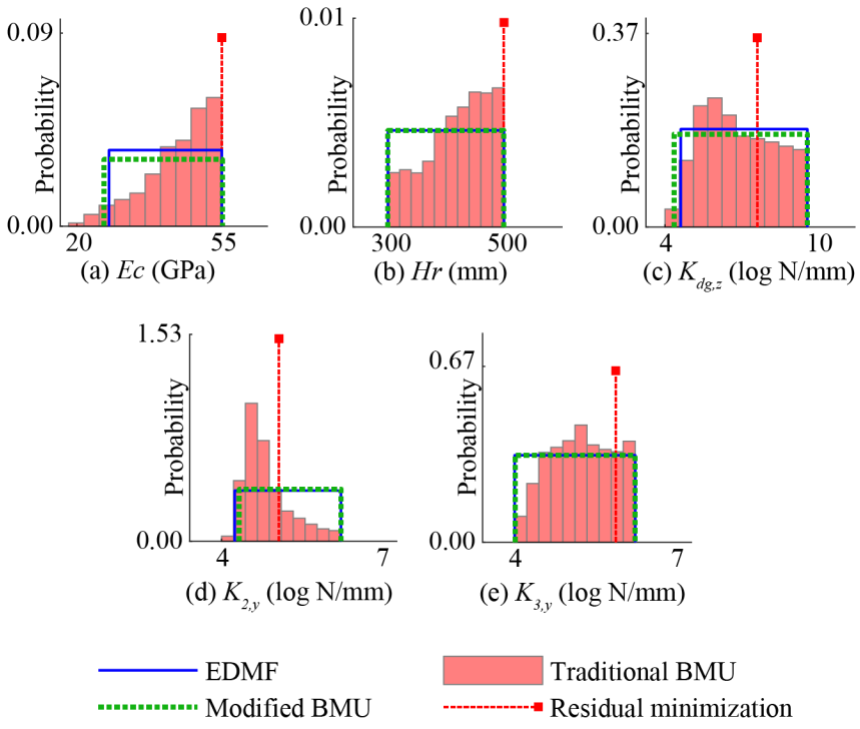

583

584 **Figure 6 Histogram of joint posterior PDF obtained using traditional BMU and optimal**
585 **parameter values obtained using residual minimization**

586 **4.4 Cross-Validation**

587 Cross-validation methods are used to assess accuracy of structural identification and validate the
588 assumptions made in uncertainty estimations. In the next few sections, validation methods, leave-
589 one-out and hold-out cross-validation for assessment of structural identification solutions, are
590 presented.

591 4.4.1 Leave-one-out cross-validation

592 In leave-one-out cross-validation, one data point among a set of *m* data points available is omitted.
593 Using the *m*-1 data points, structural identification is carried out to obtain an updated distribution
594 of model parameters. This updated model parameter distribution is then provided as input to the
595 physics-based model to predict the response at the location of the data point left out. If the updated

predictions are compatible with the omitted measurement, then structural identification is accurate for this measurement location. This process is then repeated *m* times to independently assess identification at each measurement location.

Figure 7 shows a comparison of predictions made using updated knowledge of model parameters with measurement left out. The structural identification is carried out using 7 sensors with one sensor left out for each scenario. The comparisons shown in the figure indicate that structural identification carried out using EDMF and modified BMU are accurate for every case. Residual minimization and Traditional BMU are not accurate for the case studied in Figure 7c. This is also supported by evaluations using equations (15), (16) and (17). Nevertheless, the updated predictions using all data-interpretation methodologies are comparable to the measured structural response.

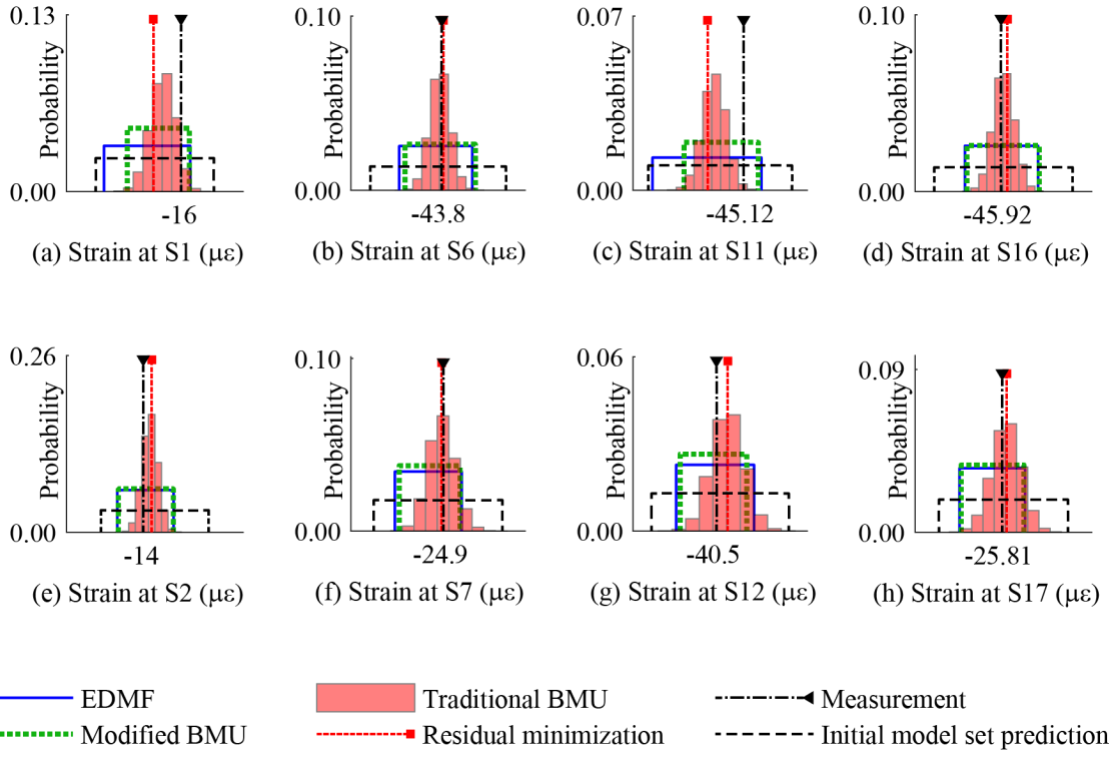

Figure 7 Leave-one-out cross validation of identification results obtained using the four data-interpretation methodologies. Based on leave-one-out cross-validation all data-interpretation methodologies provide accurate solutions for most cases.

However, an assumption made during leave-one-out cross-validation is that each data point left out provides new information that is not available in the dataset (*m-1* data points) used for identification. Exclusive information contained in data point left out (set *B*) compared with information contained in dataset for identification (set *A*) can be calculated using Eq. (21). The exclusive information contained in the sensor left out, relative to information from all 8 sensors, $H(g_{A,B})$, is shown in Figure 8.

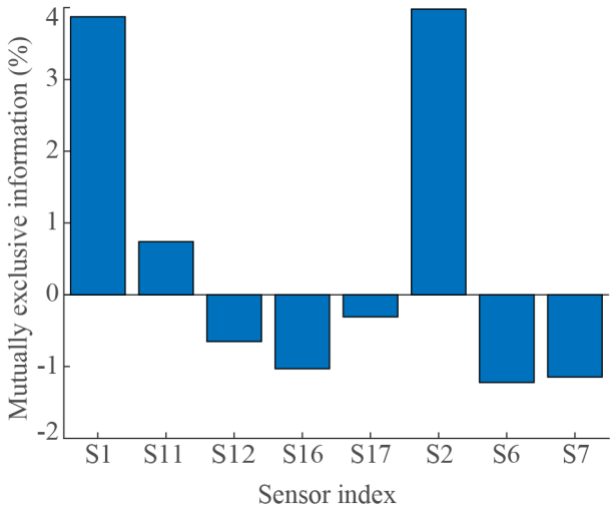

Figure 8 Exclusive information in sensor omitted for leave-one-out cross-validation. The sensors left out generally contain redundant or little new information for validation.

In Figure 8, exclusive information provided by sensor left-out compared with information from the other 7 sensors for identification for each case of leave-one-out cross-validation is shown. For most sensors, the sensor left out shows negative values, which indicates redundant information and over-instrumentation. Therefore, most sensors provide no new information for leave-one-out cross-validation. Consequently, validation with leave-one-out cross-validation is not appropriate to justify accuracy of structural identification in this situation.

4.4.2 Hold-out cross-validation

In hold-out validation, a second and independent dataset is used for validation, i.e., data that has not been used for structural identification in a similar way to training and validating artificial neural networks. Structural identification for the PMB has been carried out using data from eight strain gauges (identification set A), shown in Figure 5. In addition to these eight strain gauges, there are twelve strain gauges (validation set B), as shown in Figure 5, data from which is utilized in this section for hold-out cross-validation of structural identification solutions. Exclusive information from these twelve strain measurements compared with information from eight strain gauges is calculated using Eq. (21). This exclusive information is calculated to be 16% of the total information from the twenty measurements (8 in set A and 12 in set B) available. Figure 9 shows a comparison of updated predictions at the held-out sensor locations with measured structural response.

As shown in Figure 9, updated predictions obtained using all methodologies are not compatible with measurements at all sensor locations. EDMF and modified BMU provide accurate, albeit imprecise, prediction bounds that include the measured structural response for all sensor locations. Traditional BMU and residual minimization provide more precise updated model predictions than EDMF and modified BMU. However, the predictions are not compatible with measurements at all sensor locations (for example, see predictions at sensors S8, S9, S13, S14, S15 and S18).

Using equations (15), EDMF and modified BMU are evaluated to provide accurate updated predictions at all measurements held out (overall accuracy = 100%). Using (16), traditional BMU is evaluated to provide accurate updated predictions for only 5 out of 12 measurement locations held out (overall accuracy = 5/12*100 = 42%). Similarly, assessing accuracy using Eq. (17), residual minimization provides accurate updated predictions for only 5 out of 12 measurement

locations held out (overall accuracy = 5/12*100 = 42%). Therefore, traditional BMU and residual minimization do not provide accurate structural identification even for a relatively low amount (16%) of new information in the held-out data set.

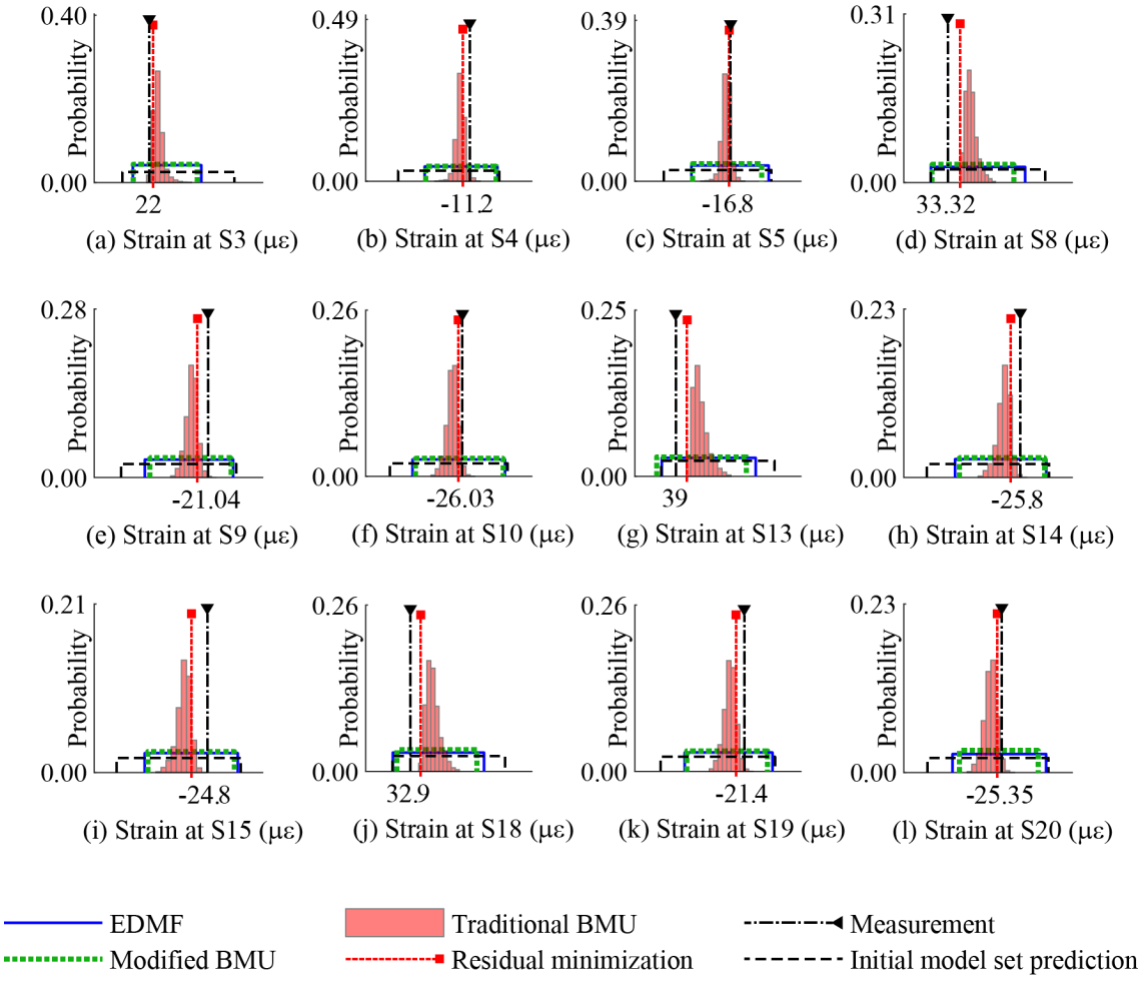

Figure 9 Hold-out cross validation of identification results obtained using the four data-interpretation methodologies. EDMF and modified BMU provide identification results that are accurate even when validated with mutually exclusive information.

4.4.3 Hold-out cross-validation using measurements from a second load test

A second load test was performed on the PMB, similar to one described in Section 4.1. During this load test, a truck weighing 33 tonnes was driven across the bridge at a speed of 10km/h. The

alignment of the truck on the bridge is shown in Figure 10. The response of the bridge to this truck loading was recorded using strain gauges placed on the lower steel beam flanges of PMB. The location of these gauges in plan view is shown in Figure 5. In total, 18 strain gauges recorded structural response during the load test.

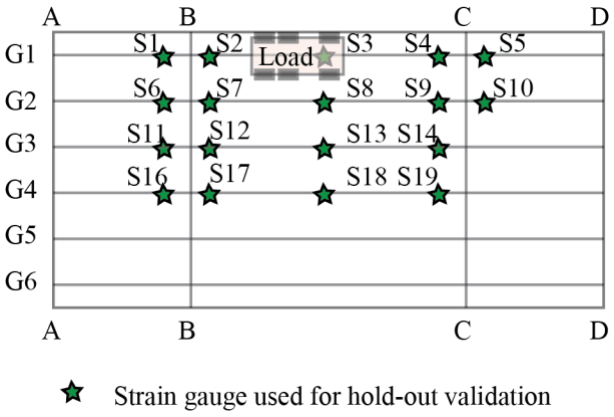

Figure 10 Plan view of second load test on the PMB showing location of 18 strain gauges and position of the truck load. Data from these strain gauges is used for cross-validation of structural identification solutions. Sensors S15 and S20 shown in Figure 5 were not working during this second load test.

Data from sensors shown in Figure 10 are held-out for cross-validation. The data utilised corresponds to the point in time when movement of the truck leads to maximum strain recorded in S13 (see Figure 10). Figure 11 shows few cases of updated predictions made at sensor locations S4, S9, S14 and S19 (strain predictions close to support C-C, see Figure 10).

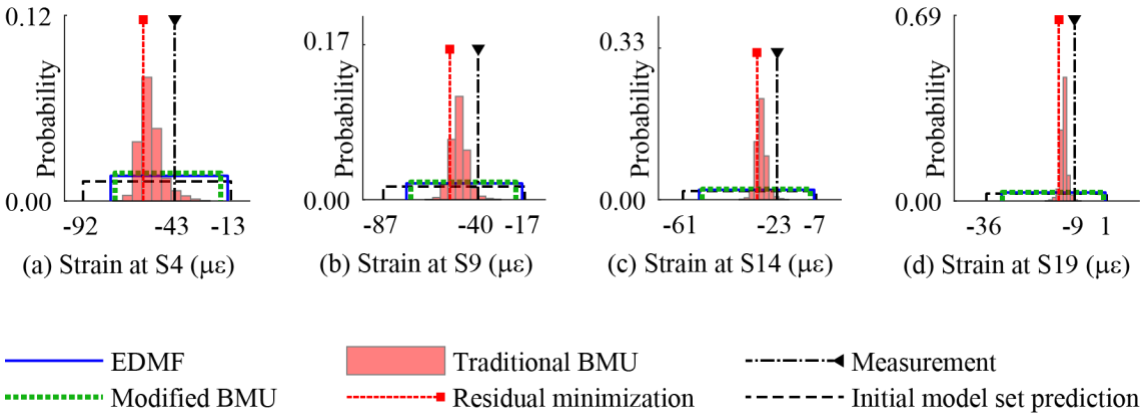

672

673 **Figure 11 Examples of holdout cross-validation using measurements from a second load test,**
674 **demonstrating inaccurate identification using traditional BMU and residual minimization.**
675 **This second load test (18 measurements) has 40% exclusive information compared with**
676 **information from load test data used for structural identification.**

677 For cases shown in Figure 11, traditional BMU and residual minimization provide precise
678 predictions (low variability), which are biased from the measured value, indicating inaccurate
679 identification. Conversely, EDMF and modified BMU provide wide bounds of predictions (large
680 prediction variability), which include the measured value and therefore provide accurate structural
681 identification. Additionally, due to similarity in solutions obtained with EDMF and modified
682 BMU, the prediction bounds obtained are also similar.

683 For the eighteen measurements used in cross-validation, traditional BMU provided accurate
684 predictions (see Eq. (16) at nine sensor locations leading to an overall accuracy of 50% (9 out of
685 18). Residual minimization is also found to provide accurate predictions (see Eq. (17) for nine out
686 of eighteen validation predictions (50% accuracy). EDMF and modified BMU provided accurate
687 predictions (see Eq. (15) for seventeen out of eighteen cases (95% accuracy).

688 EDMF and modified BMU provide accurate structural identification. Moreover, predictions
689 obtained using both methodologies are similar with differences arising only from use of different
690 sampling strategies for structural identification. In the next section, the validated structural

identification solutions have been used to predict the remaining fatigue life of a critical detail on the Powder Mill Bridge.

4.5 Remaining fatigue life prediction

Using updated model parameter distributions obtained using the application of data-interpretation methodologies, reserve capacity of PMB is predicted with respect to its RFL. The critical detail evaluated for fatigue is a welded connection located on girder G2, close to north pier (support C, near sensor S10, see Figure 9).

The category of this detail is 'C', which has a detail constant, A, of 44 ksi[3]. This detail has also been evaluated by Saberi et al. (2016). Based on in-service measurements carried out on the bridge, the average daily truck traffic (ADTT) is 255 vehicles/day. The RFL of PMB is predicted using reference manual (AASHTO 2016), as shown in Eq. (22).

$$RFL = \frac{\log\left[\frac{R_R \cdot A}{365 \cdot n \cdot ADTT \cdot [\Delta\sigma]^3} \cdot g(1+g)^{a-1} + 1\right]}{\log(1+g)} \quad \textbf{(22)}$$

In Eq. (22), R_R is the resistance factor, which is equal to 1, A is the detail constant and n is the number of cycles per truck passage, equal to 2. In the equation, g is the annual growth of traffic in percentage, which is assumed to be 1% and the variable, a, is the present age of the bridge, which during measurements was 11 years. $\Delta\sigma$ in the equation is the effective stress range (ksi). The effective stress range for PMB is computed using the FE model with the fatigue load as specified by the design code. Based on Eq. 10, the predictions of RFL are shown in Figure 12.

In Figure 12, using updated information of model parameters uncertainty in RFL prediction of the PMB is reduced. EDMF and modified BMU predict a minimum RFL of 620 and 610 years respectively. Updated model parameter distributions obtained using both these methods have been

validated using leave-one-out and hold-out cross-validation. Therefore, a minimum RFL of the PMB may be estimated to be 610 years. This value is significantly higher than the design RFL of 64 years. This reserve capacity may be utilised to guide asset-management decisions, such as replacement and possible retrofit actions due to loading changes, in the future.

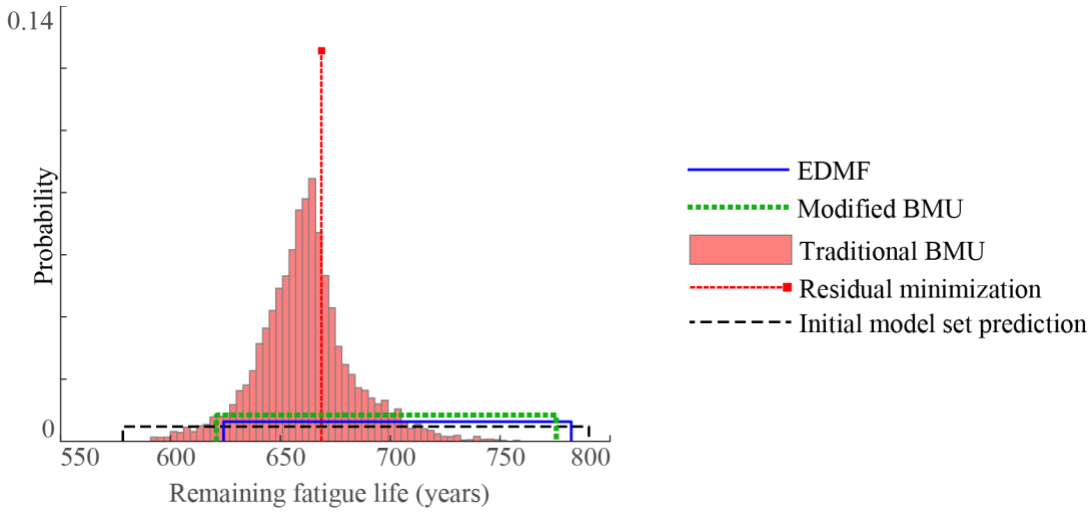

Figure 12 Updated RFL prediction of a critical welded detail using identification results obtained using the four data-interpretation methodologies. Traditional BMU and residual minimization provide a likely RFL greater than the minimum value estimated using EDMF and modified BMU. As these two methodologies are assessed to provide inaccurate structural identification, the predictions of RFL may be un-conservative for decision making.

Residual minimization and traditional BMU (using the maximum a-posteriori estimate) predict a RFL of approximately 670 years. This value is greater than the minimum RFL predicted by EDMF and modified BMU. Moreover, structural identification using residual minimization and traditional BMU has been assessed to be potentially inaccurate using hold-out cross-validation. Therefore, residual minimization and traditional BMU provide un-conservative structural identification and possibly unsafe predictions of RFL.

5. DISCUSSION

In this paper, equivalence between modified BMU and EDMF is demonstrated analytically. Modified BMU provides similar results to EDMF when applied to full-scale evaluations (see Eq. (14)), with differences arising from sampling and approximation of the box-car likelihood function (see Figure 1). Modified BMU, as shown in Figure 2, is robust to misevaluation of correlations and provides accurate results for structural identification compared with residual minimization as shown in Figure 7, Figure 9 and Figure 11. Therefore, modified BMU provides an alternative Bayesian approach for accurate structural identification, comparable with EDMF.

EDMF enables explicit quantification of uncertainties from sources that affect structural behaviour. Some of these sources are included in the model class for identification (Pai et al. 2021; Saitta et al. 2005), while others are combined together to estimate the falsification thresholds (see Eq. (4). Quantification of these uncertainties, particularly those related to the model, are based on engineering knowledge such as assumptions involved in model development, observations from site inspection and conditions of loading (Goulet et al. 2013).

Modified BMU provides the same results as EDMF. Additionally, modified BMU also allows for explicit quantification of uncertainties as part of development of model priors and the likelihood function based on falsification thresholds (see equations (12 and (13). Traditional BMU (Beck and Katafygiotis 1998) and other novel variants (Behmanesh et al. 2015; Simoen et al. 2013) do not allow for engineering knowledge to be explicitly included in development of the likelihood function. Wang and Liu (2020) have used Bayesian entropy networks to include constraints based on engineering knowledge.

Bayesian model updating requires complex strategies to sample from the posterior (Kuśmierczyk et al. 2019; Qian et al. 2003) such as MCMC sampling for accurate inference. Moreover,

752 appropriate implementation of these sampling methods and interpretation of posterior PDFs for
753 asset management requires statistical knowledge (Aczel et al. 2020). The task of asset management
754 is iterative (Pasquier and Smith 2016). Therefore, the task of model-based data interpretation needs
755 to be transparent for repeated evaluations as new information becomes available over time.
756 Iterations of data interpretation with new information may be computationally expensive using
757 sampling methods such as MCMC. These are few challenges related to practical implementation
758 of BMU. A more comprehensive discussion related to practical challenges associated with the
759 application of various data-interpretation methodologies has been carried out by Pai et al. (2019).

760 Utility of measurements to improve understanding of structural behaviour using EDMF may be
761 assessed using a cross-entropy measure (Jiang and Mahadevan 2006) to compare prior parameter
762 distributions with posterior parameter distributions.

763 Subsequent to structural identification, validation of solutions using leave-one-out and hold-out
764 cross-validation is assessed. In the absence of informative data to be withheld for validation,
765 assessment of accuracy of structural identification is not appropriate, as shown in Figure 7. Leave-
766 one-out cross-validation, with mostly redundant information, falsely suggests that all data-
767 interpretation methodologies provide accurate structural identification most of the time. This is
768 shown to be wrong when validation is carried out using the hold-out method. In the hold-out
769 method, with informative data in the validation dataset, structural identification using residual
770 minimization and traditional BMU is assessed to be inaccurate.

771 Other than leave-one-out and hold-out validation, users may also adopt the *k*-fold validation
772 (Bengio and Grandvalet 2004) strategy. In this strategy, the set of measurement data is divided
773 into *k* folds (subsets). One of these folds is used for validation, while data in *k*-1 folds is used for
774 model updating. Subsequently, the validation is performed with another fold and this process is

775 iterated till model updating is validated with all *k* folds. When *k* is set equal to number of
776 measurements available (*m*), then *k*-fold validation is essentially leave-one-out cross-validation.
777 Using this method poses challenges related to amount of data necessary and selecting the
778 appropriate value of *k* (Rodríguez et al. 2010), which affects validation accuracy.

779 Using validated solutions obtained using EDMF and modified BMU, the RFL of the Powder Mill
780 Bridge with respect to a cover plate detail is calculated. The bridge has significant reserve capacity
781 with respect to the fatigue limit state compared with design calculations. More importantly, RFL
782 predictions obtained using traditional BMU and residual minimization were greater than those
783 obtained using EDMF and modified BMU. Therefore, structural identification with inappropriate
784 uncertainty assumptions may lead to inaccurate solutions and unsafe predictions.

785 The presence of significant reserve capacity for the PMB is similar to previous observations that
786 typically indicate over-design of civil infrastructure. Smith (2016) provided a summary of case
787 studies that were evaluated to possess significant reserve capacity beyond design requirements by
788 using information obtained with monitoring. The presence of reserve capacity beyond design has
789 been observed for steel bridges (Pasquier et al. 2014, 2016) with respect to the fatigue limit state
790 (Pai et al. 2018) and concrete bridges with respect to serviceability and ultimate limit state
791 (Proverbio et al. 2018c). Reserve capacity of PMB evaluated in this study adds to existing
792 observations on over-design of civil infrastructure built with conservative and simplified models.

793 Similar over-design of civil infrastructure, due to low marginal initial costs to reduce for example,
794 construction risk, may not be acceptable in the future due to sustainability considerations and lack
795 of availability of raw materials. Better design guidelines may be necessary to minimize wastage
796 of raw materials and reduce life-cycle energy consumption. Correctly interpreting monitoring data
797 to update models provides support for improving data-enhanced design guidelines.

798 The modified BMU methodology presented in this paper and the information theoretic approach
799 adopted to perform validation of structural identification enable use of monitoring for asset
800 management. Transfer of this research into practice will require users to address additional
801 challenges related to detecting outliers in data (Proverbio et al. 2018a) and adopting efficient
802 strategies to search for solutions (Proverbio et al. 2018b; Raphael and Smith 2003).

803 The EDMF methodology relies on engineering expertise to assess uncertainty sources affecting
804 the structural system. While developments in model-class assessment and selection (Pai et al.
805 2021; Pasquier and Smith 2016) provide certain checks to ensure important sources of uncertainty
806 are addressed, site inspections and engineering knowledge are important for accurate
807 implementation of EDMF.

808 In this paper, validation has been performed for one case study. While there are no reasons why
809 similar cases cannot benefit, to ensure scalability, such validation studies have to be performed on
810 many full-scale case studies. With more evaluations, guidelines on selecting data for appropriate
811 validation and improvements in the validation strategy, such as *k*-fold validation, may be assessed.
812 With more validation studies, assessment of reserve capacity may be improved, thereby enhancing
813 asset management.

814 **6. CONCLUSIONS**

815 In this paper, three data-interpretation methodologies are compared for structural identification of
816 a steel-concrete composite bridge. Results of structural identification are verified using cross-
817 validation and they are subsequently used to predict remaining fatigue lives of the bridge structure.
818 The conclusions obtained are as follows:

- EDMF provides more accurate interpretation of measurement data using physics-based models compared with traditional BMU and residual minimization. Modifications to the likelihood function for BMU also provides accurate structural identification since the two methods become analytically equivalent.
- Verification of identification solutions using leave-one-out cross-validation is a necessary but not a sufficient condition. Leave-one-out cross-validation may lead to verification with information that is already included in identification. This is not sufficient to justify using results obtained from identification for extrapolation predictions such as those necessary to estimate reserve capacity.
- Verification of identification solutions using hold-out cross-validation is required when leave-one-out cross-validation fails to verify solutions with new information. Hold-out cross-validation with information not available during identification helps verify results obtained from identification for extrapolation predictions that are necessary to estimate reserve capacity.
- Inaccurate structural identification using traditional BMU and residual minimization, as verified using either leave-one-out or hold-out cross-validation, leads to un-conservative predictions of reserve capacity.
- Results from this paper add to a growing body of evidence that most structures possess reserve capacity well beyond design requirements. Accurate and safe quantification of this reserve capacity using data-informed physics-based models enables well informed asset management and avoids unnecessary and expensive management actions.

7. ACKNOWLEDGEMENTS

This work was funded by the Swiss National Science Foundation under contract no. 200020-169026 and the Singapore-ETH centre (SEC) under contract no. FI 370074011-370074016. These

842 grants are gratefully acknowledged. The authors would like to acknowledge J-A. Goulet, Poly.
843 Montreal, Canada, N. Bertola, EPFL, Switzerland and M. Sanayei, Tufts University, USA for
844 fruitful discussions. The authors are also grateful to M. Sanayei for providing data related to the
845 case study which is also known as the Vernon Avenue Bridge (Sanayei et al. 2011).

846 8. REFERENCES

847 Aczel, B., Hoekstra, R., Gelman, A., Wagenmakers, E. J., Klugkist, I. G., Rouder, J. N.,
848 Vandekerckhove, J., Lee, M. D., Morey, R. D., Vanpaemel, W., Dienes, Z., and van
849 Ravenzwaaij, D. (2020). "Discussion points for Bayesian inference." *Nature Human*
850 *Behaviour*, Nature Research.

851 Alvin, K. (1997). "Finite Element Model Update via Bayesian Estimation and Minimization of
852 Dynamic Residuals." *AIAA Journal*, 35(5), 879–886.

853 Amin, A.-L., and Watkins, G. (2018). "How sustainable infrastructure can help us fight climate
854 change."

855 ANSYS. (2012). *ANSYS Mechanical APDL Element Reference*.

856 APDL, A. M. (2010). "Mechanical applications Theory reference." *ANSYS Release*, 13.

857 ASCE. (2017). *Infrastructure Report Card*.

858 Atamturktur, S., Liu, Z., Cogan, S., and Juang, H. (2015). "Calibration of imprecise and inaccurate
859 numerical models considering fidelity and robustness: a multi-objective optimization-based
860 approach." *Structural and Multidisciplinary Optimization*, Springer, 51(3), 659–671.

861 Bayes, T. (1763). "LII. An essay towards solving a problem in the doctrine of chances. By the late
862 Rev. Mr. Bayes, FRS communicated by Mr. Price, in a letter to John Canton, AMFR S."

Philosophical transactions of the Royal Society of London, The Royal Society London, (53), 370–418.

Beck, J. L. (2010). "Bayesian system identification based on probability logic." *Structural Control and Health Monitoring*, Wiley Online Library, 17(7), 825–847.

Beck, J. L., Au, S.-K., and Vanik, M. W. (2001). "Monitoring structural health using a probabilistic measure." *Computer-Aided Civil and Infrastructure Engineering*, Wiley Online Library, 16(1), 1–11.

Beck, J. L., and Katafygiotis, L. S. (1998). "Updating models and their uncertainties. I: Bayesian statistical framework." *Journal of Engineering Mechanics*, 124(4), 455–461.

Behmanesh, I., Moaveni, B., Lombaert, G., and Papadimitriou, C. (2015). "Hierarchical Bayesian model updating for structural identification." *Mechanical Systems and Signal Processing*, Elsevier, 64, 360–376.

Bengio, Y., and Grandvalet, Y. (2004). "No unbiased estimator of the variance of K-fold cross-validation." *Journal of Machine Learning Research*, 5(Sep), 1089–1105.

Beven, K. J. (2000). "Uniqueness of place and process representations in hydrological modelling." *Hydrology and Earth System Sciences Discussions*, 4(2), 203–213.

Brownjohn, J. M. W., Moyo, P., Omenzetter, P., and Lu, Y. (2003). "Assessment of highway bridge upgrading by dynamic testing and finite-element model updating." *Journal of Bridge Engineering*, American Society of Civil Engineers, 8(3), 162–172.

Brownjohn, J. M. W., Xia, P.-Q., Hao, H., and Xia, Y. (2001). "Civil structure condition assessment by FE model updating:: methodology and case studies." *Finite elements in*

analysis and design, Elsevier, 37(10), 761–775.

Brynjarsdóttir, J., and O'Hagan, A. (2014). "Learning about physical parameters: The importance of model discrepancy." *Inverse Problems*, IOP Publishing, 30(11), 114007.

Van Buren, K. L., Hall, T. M., Gonzales, L. M., Hemez, F. M., and Anton, S. R. (2015). "A case study to quantify prediction bounds caused by model-form uncertainty of a portal frame." *Mechanical Systems and Signal Processing*, Elsevier, 50, 11–26.

Van Buren, K. L., Mollineaux, M. G., Hemez, F. M., and Atamturktur, S. (2013). "Simulating the dynamics of wind turbine blades: part II, model validation and uncertainty quantification." *Wind Energy*, Wiley Online Library, 16(5), 741–758.

Cao, W. J., Liu, W. S., Koh, C. G., and Smith, I. F. C. (2020). "Optimizing the operating profit of young highways using updated bridge structural capacity." *Journal of Civil Structural Health Monitoring*, Springer, 10(2), 219–234.

Chen, X., Omenzetter, P., and Beskhyroun, S. (2014). "Calibration of the finite element model of a twelve-span prestressed concrete bridge using ambient vibration data." *Proceedings of the 7th European Workshop on Structural Health Monitoring*.

Ching, J., and Beck, J. L. (2004). "New Bayesian model updating algorithm applied to a structural health monitoring benchmark." *Structural Health Monitoring*, Sage Publications Sage CA: Thousand Oaks, CA, 3(4), 313–332.

Cox, M. G., and Siebert, B. R. L. (2006). "The use of a Monte Carlo method for evaluating uncertainty and expanded uncertainty." *Metrologia*, IOP Publishing, 43(4), S178.

Drzik. (2019). "Infrastructure around the world is failing. Here's how to make it more resilient."

World Economic Forum, <https://www.weforum.org/agenda/2019/01/infrastructure-around-the-world-failing-heres-how-to-make-it-more-resilient/>.

Feng, D., and Feng, M. Q. (2015). "Model updating of railway bridge using in situ dynamic displacement measurement under trainloads." *Journal of Bridge Engineering*, American Society of Civil Engineers, 20(12), 4015019.

Follen, C. W., Sanayei, M., Brenner, B. R., and Vogel, R. M. (2014). "Statistical Bridge Signatures." *Journal of Bridge Engineering*, American Society of Civil Engineers (ASCE), 19(7), 04014022.

Friedman, J. H. (1991). "Multivariate Adaptive Regression Splines." *The Annals of Statistics*, Institute of Mathematical Statistics, 19(1), 1–67.

Gelman, A., Stern, H. S., Carlin, J. B., Dunson, D. B., Vehtari, A., and Rubin, D. B. (2013). *Bayesian data analysis*. Chapman and Hall/CRC.

Golub, G. H., Heath, M., and Wahba, G. (1979). "Generalized cross-validation as a method for choosing a good ridge parameter." *Technometrics*, 21(2), 215–223.

Goulet, J.-A. (2012). "Probabilistic model falsification for infrastructure diagnosis." *Thesis*, EPFL.

Goulet, J.-A. A., Texier, M., Michel, C., Smith, I. F. C. C., and Chouinard, L. (2013). "Quantifying the effects of modeling simplifications for structural identification of bridges." *Journal of Bridge Engineering*, American Society of Civil Engineers, 19(1), 59–71.

Goulet, J.-A., Kripakaran, P., and Smith, I. F. C. (2010). "Multimodel Structural Performance Monitoring." *Journal of Structural Engineering*, American Society of Civil Engineers, 136(10), 1309–1318.

926 Goulet, J. A., and Smith, I. F. C. (2013). “Structural identification with systematic errors and
927 unknown uncertainty dependencies.” *Computers and Structures*, Elsevier, 128, 251–258.

928 Hashemi, S. M., and Rahmani, I. (2018). “Determination of Multilayer Soil Strength Parameters
929 Using Genetic Algorithm.” *Civil Engineering Journal*, 4(10), 2383–2397.

930 Hong, Y. M., and Wan, S. (2011). “Information-based system identification for predicting the
931 groundwater-level fluctuations of hillslopes.” *Hydrogeology Journal*, Springer, 19(6), 1135–
932 1149.

933 Huang, Y., Beck, J. L., and Li, H. (2017). “Bayesian system identification based on hierarchical
934 sparse Bayesian learning and Gibbs sampling with application to structural damage
935 assessment.” *Computer Methods in Applied Mechanics and Engineering*, Elsevier, 318, 382–
936 411.

937 Jaynes, E. T. (1957). “Information theory and statistical mechanics.” *Physical review*, APS,
938 106(4), 620.

939 Jiang, X., and Mahadevan, S. (2006). “Bayesian cross-entropy methodology for optimal design of
940 validation experiments Related content Optimal Design of Validation Experiments Based on
941 Area Metric Factor and Fuzzy Expert System Bin Suo et al-Special issue: a comprehensive
942 study on enhanced optimization-based model calibration using gradient information Bayesian
943 cross-entropy methodology for optimal design of validation experiments.” *Meas. Sci.*
944 *Technol*, 17, 1895–1908.

945 Jiang, X., and Mahadevan, S. (2008). “Bayesian validation assessment of multivariate
946 computational models.” *Journal of Applied Statistics*, Taylor & Francis, 35(1), 49–65.

947 Katafygiotis, L. S., and Beck, J. L. (1998). “Updating Models and Their Uncertainties. II: Model

948 Identifiability." *Journal of Engineering Mechanics*, American Society of Civil Engineers,
949 124(4), 463–467.

950 Katafygiotis, L. S., Papadimitriou, C., and Lam, H.-F. (1998). "A probabilistic approach to
951 structural model updating." *Soil Dynamics and Earthquake Engineering*, Elsevier, 17(7–8),
952 495–507.

953 Kennedy, M. C., and O'Hagan, A. (2001). "Bayesian calibration of computer models." *Journal of*
954 *the Royal Statistical Society: Series B (Statistical Methodology)*, Wiley Online Library, 63(3),
955 425–464.

956 Koh, C. G., and Zhang, Z. (2013). "The Use of Genetic Algorithms for Structural Identification
957 and Damage Assessment." *Health Assessment of Engineered Structures: Bridges, Buildings*
958 *and Other Infrastructures*, World Scientific, 241–267.

959 Kohavi, R., and others. (1995). "A study of cross-validation and bootstrap for accuracy estimation
960 and model selection." *International Joint Conference on Artificial Intelligence (IJCAI)*,
961 1137–1145.

962 Kuok, S.-C. C., and Yuen, K.-V. V. (2016). "Investigation of modal identification and modal
963 identifiability of a cable-stayed bridge with Bayesian framework." *Smart Structures and*
964 *Systems*, 17(3), 445–470.

965 Kuśmierczyk, T., Sakaya, J., and Klami, A. (2019). "Correcting Predictions for Approximate
966 Bayesian Inference."

967 Kwon, K., Frangopol, D. M., and Kim, S. (2013). "Fatigue performance assessment and service
968 life prediction of high-speed ship structures based on probabilistic lifetime sea loads."
969 *Structure and Infrastructure Engineering*, Taylor & Francis, 9(2), 102–115.

970 Levasseur, S., Malécot, Y., Boulon, M., and Flavigny, E. (2008). “Soil parameter identification
971 using a genetic algorithm.” *International Journal for Numerical and Analytical Methods in*
972 *Geomechanics*, Wiley Online Library, 32(2), 189–213.

973 Ljung, L. (2010). “Perspective on System Identification.” *Annual Reviews in Control*, Elsevier,
974 34(1), 1–12.

975 Majumdar, A., Maiti, D. K., and Maity, D. (2012). “Damage assessment of truss structures from
976 changes in natural frequencies using ant colony optimization.” *Applied mathematics and*
977 *computation*, Elsevier, 218(19), 9759–9772.

978 Matos, J. C., Cruz, P. J. S., Valente, I. B., Neves, C. ., Moreira, V. N., Neves, L. C., and Moreira,
979 V. N. (2016). “An innovative framework for probabilistic-based structural assessment with
980 an application to existing reinforced concrete structures.” *Engineering Structures*, 111, 552–
981 564.

982 McFarland, J., and Mahadevan, S. (2008). “Multivariate significance testing and model calibration
983 under uncertainty.” *Computer methods in applied mechanics and engineering*, Elsevier,
984 197(29–32), 2467–2479.

985 McKay, M. D., Beckman, R. J., and Conover, W. J. (1979). “A Comparison of Three Methods for
986 Selecting Values of Input Variables in the Analysis of Output from a Computer Code.”
987 *Technometrics*, JSTOR, 21(2), 239.

988 Moon, F., Catbas, N., Çatba\cs, F. N., Kijewski-Correa, T., Aktan, A. E., Çatbaş, F. N., Kijewski-
989 Correa, T., and Aktan, A. E. (2013). “Structural Identification of Constructed Systems.”
990 *Structural Identification of Constructed Systems*, American Society of Civil Engineers, 1–17.

991 Mosavi, A. A., Sedarat, H., O’Connor, S. M., Emami-Naeini, A., and Lynch, J. (2014).

992 “Calibrating a high-fidelity finite element model of a highway bridge using a multi-variable
993 sensitivity-based optimisation approach.” *Structure and Infrastructure Engineering*, Taylor
994 & Francis, 10(5), 627–642.

995 Mottershead, J. E., and Friswell, M. I. (1993). “Model updating in structural dynamics: A survey.”
996 *Journal of Sound and Vibration*, 167(2), 347–375.

997 Mottershead, J. E. J. E., Link, M., and Friswell, M. I. M. I. (2011). “The sensitivity method in
998 finite element model updating: a tutorial.” *Mechanical Systems and Signal Processing*,
999 Elsevier, 25(7), 2275–2296.

1000 Muto, M., and Beck, J. L. (2008). “Bayesian updating and model class selection for hysteretic
1001 structural models using stochastic simulation.” *Journal of Vibration and Control*, SAGE
1002 Publications, 14(1–2), 7–34.

1003 Nanda, B., Maity, D., and Maiti, D. K. (2014). “Modal parameter based inverse approach for
1004 structural joint damage assessment using unified particle swarm optimization.” *Applied*
1005 *Mathematics and Computation*, Elsevier, 242, 407–422.

1006 Neumann, M. B., and Gujer, W. (2008). “Underestimation of uncertainty in statistical regression
1007 of environmental models: influence of model structure uncertainty.” *Environmental science*
1008 *& technology*, ACS Publications, 42(11), 4037–4043.

1009 Pai, S. G. S., Nussbaumer, A., and Smith, I. F. C. (2018). “Comparing Structural Identification
1010 Methodologies for Fatigue Life Prediction of a Highway Bridge.” *Frontiers in Built*
1011 *Environment*, Frontiers, 3(73), 73.

1012 Pai, S. G. S., Reuland, Y., and Smith, I. F. C. (2019). “Data-Interpretation Methodologies for
1013 Practical Asset-Management.” *Journal of Sensor and Actuator Networks*, 8(2), 36.

Pai, S. G. S., Sanayei, M., and Smith, I. F. C. (2021). "Model-Class Selection Using Clustering and Classification for Structural Identification and Prediction." *Journal of Computing in Civil Engineering*, 35(1).

Pai, S. G. S., and Smith, I. F. C. (2017). "Comparing Three Methodologies for System Identification and Prediction." *14th International Probabilistic Workshop*, R. Caspeele, L. Taerwe, and D. Proske, eds., Springer International Publishing, Cham, 81–95.

Papadimitriou, C., Beck, J. L., and Au, S.-K. (2000). "Entropy-Based Optimal Sensor Location for Structural Model Updating." *Journal of Vibration and Control*, Sage Publications, 6(5), 781–800.

Papadimitriou, C., Beck, J. L., and Katafygiotis, L. S. (2001). "Updating robust reliability using spectral test data." *Probabilistic Engineering Mechanics*, Elsevier, 16(2), 103–113.

Papadopoulou, M., Raphael, B., Smith, I. F. C., and Sekhar, C. (2014). "Hierarchical Sensor Placement Using Joint Entropy and the Effect of Modeling Error." *Entropy*, 16, 5078–5101.

Pasquier, R., D'Angelo, L., Goulet, J.-A., Acevedo, C., Nussbaumer, A., and Smith, I. F. C. (2016). "Measurement, Data Interpretation, and Uncertainty Propagation for Fatigue Assessments of Structures." *Journal of Bridge Engineering*, American Society of Civil Engineers, 21(5), 04015087.

Pasquier, R., Goulet, J.-A., Acevedo, C., and Smith, I. F. C. (2014). "Improving Fatigue Evaluations of Structures Using In-Service Behavior Measurement Data." *Journal of Bridge Engineering*, American Society of Civil Engineers, 19(11), 04014045.

Pasquier, R., and Smith, I. F. C. (2015). "Robust system identification and model predictions in the presence of systematic uncertainty." *Advanced Engineering Informatics*, Elsevier, 29(4),

1036 1096–1109.

1037 Pasquier, R., and Smith, I. F. C. (2016). “Iterative structural identification framework for
1038 evaluation of existing structures.” *Engineering Structures*, 106, 179–194.

1039 Popper, K. (1959). *The logic of scientific discovery*. *The Logic of Scientific Discovery*.

1040 Proverbio, M., Bertola, N. J., and Smith, I. F. C. (2018a). “Outlier-detection methodology for
1041 structural identification using sparse static measurements.” *Sensors (Switzerland)*, 18(6).

1042 Proverbio, M., Costa, A., and Smith, I. F. (2018b). *Adaptive sampling methodology for structural
1043 identification using radial basis functions*. *J of Computing in Civil Engineering*.

1044 Proverbio, M., Vernay, D. G., and Smith, I. F. C. (2018c). “Population-based structural
1045 identification for reserve-capacity assessment of existing bridges.” *Journal of Civil Structural
1046 Health Monitoring*, Springer Verlag, 8(3), 363–382.

1047 Qian, S. S., Stow, C. A., and Borsuk, M. E. (2003). “On Monte Carlo methods for Bayesian
1048 inference.” *Ecological Modelling*, 159(2–3), 269–277.

1049 Raphael, B., and Smith, I. F. C. (2003). “A direct stochastic algorithm for global search.” *Applied
1050 Mathematics and Computation*, Elsevier, 146(2–3), 729–758.

1051 Rebba, R., and Mahadevan, S. (2006). “Validation of models with multivariate output.” *Reliability
1052 Engineering & System Safety*, Elsevier, 91(8), 861–871.

1053 Rechea, C., Levasseur, S., and Finno, R. (2008). “Inverse analysis techniques for parameter
1054 identification in simulation of excavation support systems.” *Computers and Geotechnics*,
1055 Elsevier, 35(3), 331–345.

1056 Reuland, Y., Lestuzzi, P., and Smith, I. F. C. (2017). “Data-interpretation methodologies for non-

linear earthquake response predictions of damaged structures." *Frontiers in Built Environment*, Frontiers Media S.A., 3.

Robert-Nicoud, Y., Raphael, B., and Smith, I. F. C. (2005). "Configuration of measurement systems using Shannon's entropy function." *Computers and Structures*, Pergamon, 83(8–9), 599–612.

Rodríguez, J. D., Pérez, A., and Lozano, J. A. (2010). "Sensitivity Analysis of k-Fold Cross Validation in Prediction Error Estimation." *IEEE Transactions on Pattern Analysis and Machine Intelligence*, 32(3), 569–575.

Saitta, S., Raphael, B., and Smith, I. F. C. (2005). "Data mining techniques for improving the reliability of system identification." *Advanced Engineering Informatics*, Elsevier, 19(4), 289–298.

Sanayei, M., Imbaro, G., McClain, J., and Brown, L. (1997). "Structural Model Updating Using Experimental Static Measurements." *Journal of Structural Engineering*, American Society of Civil Engineers, 123(6), 792–798.

Sanayei, M., Khaloo, A., Gul, M., and Catbas, F. N. (2015). "Automated finite element model updating of a scale bridge model using measured static and modal test data." *Engineering Structures*, Elsevier, 102, 66–79.

Sanayei, M., Phelps, J. E., Sipple, J. D., Bell, E. S., and Brenner, B. R. (2011). "Instrumentation, nondestructive testing, and finite-element model updating for bridge evaluation using strain measurements." *Journal of bridge engineering*, American Society of Civil Engineers, 17(1), 130–138.

Schwer, L. E. (2007). "An overview of the PTC 60/V&V 10: Guide for verification and validation

in computational solid mechanics: Transmitted by L. E. Schwer, Chair PTC 60V&V 10." *Engineering with Computers*, 245–252.

Sidak, Z. (1967). "Rectangular confidence region for the means of multivariate normal distributions." *Journal of the American Statistical Association*, Taylor & Francis Group, 62(318), 626–633.

Simoen, E., Papadimitriou, C., and Lombaert, G. (2013). "On prediction error correlation in Bayesian model updating." *Journal of Sound and Vibration*, Elsevier, 332(18), 4136–4152.

Simoen, E., Roeck, G. De, Lombaert, G., De Roeck, G., and Lombaert, G. (2015). "Dealing with uncertainty in model updating for damage assessment: A review." *Mechanical Systems and Signal Processing*, Elsevier, 56, 123–149.

Smith, I. F. C. (2016). "Studies of Sensor Data Interpretation for Asset Management of the Built Environment." *Frontiers in Built Environment*, Frontiers, 2, 8.

Soize, C. (2010). "Generalized probabilistic approach of uncertainties in computational dynamics using random matrices and polynomial chaos decompositions." *International Journal for Numerical Methods in Engineering*, Wiley Online Library, 81(8), 939–970.

Soize, C. (2012). "Stochastic models of uncertainties in computational structural dynamics and structural acoustics." *Nondeterministic Mechanics*, Springer, 61–113.

Sorenson, H. W. (1970). "Least-squares estimation: from Gauss to Kalman." *IEEE spectrum*, IEEE, 7(7), 63–68.

Tanner, M. A. (2012). *Tools for statistical inference*. Springer-Verlag.

Tarantola, a. (2005). *Inverse problem theory and methods for model parameter estimation*. *Society*

for Industrial and Applied Mathematics, Society for Industrial and Applied Mathematics (SIAM), Philadelphia, USa.

Vernay, D. G., Favre, F.-X., and Smith, I. F. C. (2018). "Robust model updating methodology for estimating worst-case load capacity of existing bridges." *Journal of Civil Structural Health Monitoring*, 8(5), 773–790.

Walker, W. E., Harremoës, P., Rotmans, J., Van Der Sluijs, J. P., Van Asselt, M. B. A., Janssen, P., and von Krauss, M. P. (2003). "Defining uncertainty: a conceptual basis for uncertainty management in model-based decision support." *Integrated assessment*, Taylor & Francis, 4(1), 5–17.

Wang, Y., and Liu, Y. (2020). "Bayesian entropy network for fusion of different types of information." *Reliability Engineering and System Safety*, Elsevier Ltd, 195, 106747.

World Economic Forum. (2014). *Strategic Infrastructure Steps to Operate and Maintain Infrastructure Efficiently and Effectively*. Geneva.

World Economic Forum, and Boston Consulting Group. (2018). *Future Scenarios and Implications for the Industry*. Davos.

Yuen, K.-V., Beck, J. L., and Katafygiotis, L. S. (2006). "Efficient model updating and health monitoring methodology using incomplete modal data without mode matching." *Structural Control and Health Monitoring: The Official Journal of the International Association for Structural Control and Monitoring and of the European Association for the Control of Structures*, Wiley Online Library, 13(1), 91–107.

Zhang, Y., Gallipoli, D., and Augarde, C. (2013). "Parameter identification for elasto-plastic modelling of unsaturated soils from pressuremeter tests by parallel modified particle swarm

optimization.” *Computers and Geotechnics*, Elsevier, 48, 293–303.